Biotic and abiotic degradation of suspended particulate lipids along a transect in the Chukchi Sea

Jean-Francois Rontani, Lukas Smik, Sun-Yong Ha, Jun-Oh Min, Simon Belt

Biotic and abiotic degradation of suspended particulate lipids along a transect in the Chukchi Sea

Rontani, Jean-François[1*], Smik, Lukas[2], Ha, Sun-Yong[3], Min, Jun-oh[3,4], Belt, Simon T.[2]

[1] *Aix Marseille Université, Université de Toulon, CNRS/INSU/IRD, Mediterranean Institute of Oceanography (MIO), UM 110, 13288 Marseille, France.*

[2] *Biogeochemistry Research Centre, School of Geography, Earth and Environmental Sciences, University of Plymouth, Drake Circus, Plymouth, Devon PL4 8AA, UK.*

[3] *Division of Ocean Sciences, Korea Polar Research Institute, 26 Songdomirae-ro, Incheon, 21990, Republic of Korea.*

[4] *Department of Marine Science and Convergence Technology, Hanyang University, 55 Hanyangdaehak-ro, Ansan, 15588, Republic of Korea.*

* Corresponding author. Tel.: +33-4-86-09-06-02; fax: +33-4-91-82-96-41. E-mail address: jean-francois.rontani@mio.osupytheas.fr (J.-F. Rontani)

Abstract. Lipids and their degradation products were investigated in samples of suspended particulate matter (SPM) collected in summer 2015 from surface waters of a South-North transect (ca. 65–81°N) of the Chukchi Sea. This material appeared to be composed mainly of diatoms (dominated by Thalassiosirales) and copepod faecal pellet debris. The high solar irradiances measured in the surface waters (up to 500 W m^{-2}) favour chlorophyll (sensitizer) photobleaching at the expense of Type II photosensitized oxidation of unsaturated lipid components of phyto- and zooplankton (photodynamic effect). The weak photoreactivity of wax esters of herbivorous zooplankton in these SPM samples contrasts with previous observations of strong photooxidation of these compounds in sinking particles, which suggests that the photodynamic effect should be favoured in large faecal pellets of herbivorous copepods sinking quickly in weakly irradiated zones. Autoxidation (free radical induced oxidation) processes operating in all oxic environments appeared to be particularly efficient in faecal pellets of omnivorous and carnivorous zooplankton and limited in those of herbivorous origin. These differences were attributed to the consumption of algal antioxidants (such as mycosporine-like amino acids and carotenoids) during the diet of omnivorous and carnivorous copepods, favouring the involvement of free radical oxidation processes.

Key words: Chukchi Sea; SPM; Lipids; Biotic and abiotic oxidation.

1. Introduction

The Arctic and Antarctic represent the most sensitive regions on Earth in terms of responses to climate change induced by global warming (IPCC, 2013). Sea ice is a particularly characteristic feature of the polar regions and has various roles in controlling local and global climate. During recent decades, there have been dramatic changes in Arctic sea ice cover and thickness (Comiso et al., 2008), and these likely impact the local, regional and global climate through complex coupling mechanisms within the Earth system. Sea ice is also critical for polar ecosystems, providing a host for phototrophic organisms at the base of the food chain, a source of nutrients for other phototrophs, which provide food to primary consumers, and a physical platform for apex marine predators such as polar bears.

Sea ice undergoes large seasonal and inter-annual variation. Having reached its maximum extent during late winter, the region of open ocean defined by the retreating ice edge in spring/summer is frequently referred to as the marginal ice zone (MIZ). The MIZ plays host to major spring phytoplankton blooms, stimulated by higher irradiance, elevated nutrient supply and water column stratification. Such spring primary production (PP) in the MIZ drives the Arctic ecosystem and also contributes significantly to the overall carbon cycle by exerting control over atmospheric CO_2 drawdown and subsequent carbon sequestration in marine sediments (Wassman et al., 2008). Increased spatial extent and duration of open waters due to sea ice loss favors phototrophic activity, and likely explains some of the recent increase in PP in the Arctic (Arrigo et al., 2015).

Some of the most dramatic sea ice decline is evident in the MIZ of the Barents Sea, the Chukchi Sea, the Sea of Okhotsk and Baffin Bay (Onarheim et al., 2018), with impacts on both climate and ecology (Serreze et al., 2007; Leu et al., 2011; Post et al., 2013; Renaut et al., 2018). Indeed, the Chukchi Sea is generally considered as one of the most biologically productive regions in the world's oceans (Springer and McRoy, 1993). The hydrography of the Chukchi

Sea is strongly influenced by the advection of water masses from the Bering Sea (Grebmeier et al., 2006), which is particularly strong in summer (Hunt et al., 2013). This inflow of warmer waters has increased in recent times as a response to global warming, with consequences for the spatial coverage of sea ice and timing of retreat (Grebmeier et al., 2006). It is thus very important to study the lower trophic levels in this region, in order to improve our understanding of the effects of sea ice reduction on marine ecosystems (Abe et al., 2020).

In the Southern Chukchi Sea, low grazing pressure (resulting from a temporal mismatch between zooplankton and phytoplankton production; Kitamura et al., 2017), fast sinking rates of large diatoms, and shallow bottom depths (Grebmeier et al., 1988, 2006a), result in strong pelagic-benthic coupling leading to increased efficiency of carbon sinking (Bates, 2006; Chen and Borges, 2009). However, these ecosystems are currently undergoing rapid and profound changes due to the effects of climate change, which can modify the ecosystem structure from pelagic-benthic to pelagic-pelagic type structures (Piepenburg, 2005). In the present work, we aimed to monitor phytoplanktonic diversity and degradation state in different suspended particulate matter (SPM) samples collected in summer surface waters across a South-North transect in the Chukchi Sea. For this, we analysed for various lipids and their biotic and abiotic degradation products, owing to their relative stability, specificity, and general suitability as tracers of the origin and fate of organic matter (OM) (Volkman et al., 1998). Moreover, the majority of studies dealing with the degradation of phytoplanktonic OM to date have focused on biotic degradation processes (Afi et al., 1996; Sun et al., 1999; Mäkinen et al., 2017), while the role played by photooxidation and free radical-mediated oxidation (autoxidation) processes in the degradation of lipid components during the senescence of phototrophic organisms has only very recently been investigated (Rontani, 2012; Rontani and Belt, 2020).

2. Material and methods

2.1. Sampling

Seawater sampling was carried out at 14 station over the Chukchi Sea (Table S1) during Korea research ice breaker R/V *Araon* cruise (ARA06B, August 1-22, 2015). A volume of 50-100 L of seawater was directly collected into 50 L carboy bottles from the vessels underway pumped system located at about 5 m below sea level. Filtration on GF/F filters (pre-combusted at 450°C for 6 h before use to avoid contamination) was performed at sea. The samples were frozen on-board (-20°C), freeze dried in the Korean laboratory and then shipped frozen to the UK and French laboratories.

2.2. Lipid extraction

Filters were reduced at room temperature with excess $NaBH_4$ (70 mg) after adding MeOH (25 mL, 30 min) to reduce labile hydroperoxides (resulting from photo- or autoxidation) to alcohols, which are more amenable to analysis by gas chromatography (GC). A test carried out with methyl oleate confirmed that the conversion of esters to the corresponding *n*-alcohols during the $NaBH_4$ reduction step of the treatment was negligible (amount of octadec-9-en-1-ol formed < 1% of the initial methyl oleate) and could not interfere with *n*-alkan-1-ol quantification in the different samples. Water (25 mL) and KOH (2.8 g) were then added and the resulting mixture saponified by refluxing (2 h). After cooling, the mixture was acidified (HCl, 2 N) to pH 1 and extracted with dichloromethane (DCM; 3 × 20 mL). The combined DCM extracts were dried over anhydrous Na_2SO_4, filtered, and concentrated by rotary evaporation at 40°C to give total lipid extracts (TLEs).

2.3. Silylation

Dry TLEs and standards were derivatized by dissolving them in 300 µL pyridine/bis-(trimethylsilyl)trifluoroacetamide (BSTFA; Supelco; 2:1, v/v) and silylated in a heating block (50 °C, 1 h). After evaporation to dryness under a stream of N_2, the derivatized residue was dissolved in ethyl acetate/BSTFA (to avoid desilylation) and analysed by GC-QTOF.

2.4. Gas chromatography-EI quadrupole time-of-flight mass spectrometry

Accurate mass measurements were made in full scan mode using an Agilent 7890B/7200 GC/QTOF system (Agilent Technologies, Parc Technopolis – ZA Courtaboeuf, Les Ulis, France). A cross-linked 5% phenyl-methylpolysiloxane (Agilent Technologies; HP-5MS Ultra inert, 30 m × 0.25 mm, 0.25 µm film thickness) capillary column was used. Analyses were performed with an injector operating in pulsed splitless mode set at 270 °C. Oven temperature was ramped from 70 °C to 130 °C at 20 °C min^{-1} and then to 300 °C at 5 °C min^{-1}. The pressure of the carrier gas (He) was maintained at 0.69×10^5 Pa until the end of the temperature program. Instrument temperatures were 300 °C for transfer line and 230 °C for the ion source. Nitrogen (1.5 mL min^{-1}) was used as collision gas. Accurate mass spectra were recorded across the range *m/z* 50–700 at 4 GHz with the collision gas opened. The QTOF-MS instrument provided a typical resolution ranging from 8009 to 12252 from *m/z* 68.9955 to 501.9706. Perfluorotributylamine (PFTBA) was used for daily MS calibration. Compounds were identified by comparing their TOF mass spectra, accurate masses and retention times with those of standards. Quantification of each compound involved extraction of specific accurate fragment ions, peak integration, and determination of individual response factors using external standards and Mass Hunter software (Agilent Technologies, Parc Technopolis – ZA Courtaboeuf, Les Ulis, France). Saturated (SFAs) and monounsaturated fatty acids (MUFAs) were quantified with structurally similar elaidic and nonadecanoic acid standards, respectively,

and the other lipids with an exact standard. The limit of detection (LOD) for each compound was based on a signal-to-noise ratio (S/N) greater than 5. The linear range was determined using values that met the standard analysis criteria of less than 15% deviation across the concentration range. Linear responses (depending on the nature of the silylated analytes) were obtained over 2-3 orders of magnitude.

The recovery efficiency of polyunsaturated fatty acids (PUFAs) for the sample treatment was checked with a standard of $C_{20:5}$ fatty acid and compared to that obtained for the $C_{18:1\Delta9}$ (oleic) acid. Using this approach, we estimate the efficiency of $C_{20:5}$ fatty acid to be ca. 70% compared to that of oleic acid. The sample treatment employed thus induces some losses (likely thermal) of PUFAs.

2.5. Chlorophyll-a analyses

The chlorophyll-*a* (Chl-*a*) concentration was determined onboard using a Trilogy fluorometer (Turner Designs, USA) after 24 h extraction in 90 % acetone at 4°C (Parsons et al., 1984). Chl *a* was measured at 0 and 10 m and we took the mean value to represent the samples collected via the ship's underway system (ca. 5 m).

2.6. Standard compounds

Phytol, fatty acids, most of the sterols and 2,6,10,14-tetramethylpentadecanoic acid (pristanic acid) were purchased from Sigma-Aldrich (St. Quentin Fallavier, France). 6,10,14-Trimethylpentadecan-2-ol was obtained after oxidation of phytol with $KMnO_4$ in acetone (Cason and Graham, 1965) and subsequent $NaBH_4$ reduction of the resulting ketone. The syntheses of 3-methylidene-7,11,15-trimethylhexadecan-1,2-diol (phytyldiol), 3,7,11,15-tetramethylhexadec-2(*Z/E*)-en-1,4-diols and 3,7,11,15-tetramethylhexadec-3(*Z/E*)-en-1,2-diols

were described previously by Rontani and Aubert (2005). 4,8,12-Trimethyltridecanoic acid (4,8,12-TMTD acid) was synthesized from isophytol (Interchim, Montluçon, France) by a previously described procedure (Rontani et al., 1991). 3,7,11,15-Tetramethylhexadecanoic acid (phytanic acid) was produced in three steps from phytol as described previously (Rontani et al., 2003). 3,7,11,15-Tetramethylhexadecan-1-ol (dihydrophytol) was obtained by hydrogenation of phytol in methanol with Pd-$CaCO_3$ as a catalyst (Rontani et al., 2003). Type-II photosensitized oxidation of monounsaturated fatty acids and alken-1-ols was carried out in pyridine with hematoporphyrin as sensitizer, while autoxidation was achieved using Fe^{2+}/ascorbate (Loidl-Stahlhofen and Spiteller, 1994). Subsequent reduction of the resulting hydroperoxides in methanol with excess $NaBH_4$ afforded the corresponding hydroxyacids.

2.7. Determination of the double bond position of monounsaturated fatty acids and n-alken-1-ols

The double bond positions of monounsaturated fatty acids (MUFAs) were determined via analysis of the TMS derivatives of their oxidation products (allylic hydroxyacids), which are ubiquitous in environmental samples (for a review see Rontani and Belt, 2020). Silylated hydroxyacids affording di-functionalized fragment ions upon electron ionization (EI) (Fig. 2) were selected for this purpose. Monitoring of the accurate mass of these fragment ions (Table S2) allowed an unambiguous assignment of the double bond position of the MUFAs present in the samples investigated (an example is given in Fig. 2). It may be noted that these double bond positions may also be identified (although less clear) by GC-MS using unit masses. However, in the case of *n*-alken-1-ols, the use of accurate masses (Table S3) is needed (Fig. 3). Indeed, unit masses of the fragment ions arising from EI fragmentation of the TMS derivatives of *n*-alken-1-ol oxidation products (diols) interfere with more stable isobaric fragment ions arising

from the fragmentation of oxidation products of some MUFAs, which are present in higher proportions than *n*-alken-1-ols in environmental samples.

This straightforward method for determining double bond positions only requires adding a simple $NaBH_4$ reduction step (to reduce unstable hydroperoxyacids to the corresponding hydroxyacids; Marchand and Rontani, 2001) prior to alkaline hydrolysis, which is commonly employed for the treatment of complex lipid extracts (Volkman, 2006).

2.8. Chlorophyll photooxidation estimates

Type II photosensitized oxidation of the chlorophyll phytyl side-chain leads to the production of 2-hydroperoxy-3-methylidene-7,11,15-trimethylhexadecan-1-ol, which, after $NaBH_4$ reduction, is converted to 3-methylidene-7,11,15-trimethylhexadecan-1,2-diol (phytyldiol) (Rontani et al., 1994). This diol constitutes a stable and specific tracer for the photodegradation of the chlorophyll phytyl side-chain (Cuny and Rontani, 1999). The molar ratio phytyldiol:phytol (Chlorophyll Phytyl side-chain Photodegradation Index, CPPI) has been previously proposed to estimate the extent of photodegradation of chlorophylls possessing a phytyl side-chain through use of the empirical equation: chlorophyll photodegradation % = $(1 - [CPPI + 1]^{-18.5}) \times 100$ (Cuny et al., 1999)' this equation was employed previously in natural marine samples from various latitudes (For reviews see Rontani and Belt, 2020; Rontani et al., 2021).

2.9. Lipid photo- and autoxidation estimates

Type-II photosensitized oxidation of Δ^5-sterols produces mainly unstable Δ^6-5α-hydroperoxides with smaller amounts of stable and specific Δ^4-6α/6β-hydroperoxides (Kulig and Smith, 1973). Sterol photooxidation percentage can be estimated on the basis of Δ^4-

3β,6α/β-dihydroxysterols (arising from $NaBH_4$ reduction of the corresponding hydroperoxides) concentration using the equation: sterol photooxidation % = (Δ^4-3β,6α/β-dihydroxysterol %) × (1+0.3)/0.3 (Christodoulou et al., 2009), where the value (0.3) corresponds to the ratio Δ^4-6α/β-hydroperoxides/Δ^6-5α-hydroperoxides found in biological membranes (Korytowski et al., 1992). Free radical autoxidation of Δ^5-stenols yields mainly unstable and unspecific 7α-and 7β-hydroperoxides and, to a lesser extent, specific 5α/β,6α/β-epoxysterols and their stable hydrolysis products 3β,5α,6β-trihydroxysterols (Smith, 1981). The extent of sterol autoxidation can be estimated after alkaline hydrolysis using the equation: sterol autoxidation % = (3ß,5α,6β-trihydroxysterols %) × 2.4 based on respective formation rate constants of the different autoxidation products obtained from incubation experiments (Christodoulou et al., 2010) and calculated previously by Morrisey and Kiely (2006). These equations have been employed previously to obtain reliable estimates of sterol photo- and autoxidation in various marine areas (For reviews see Rontani and Belt, 2020; Rontani et al., 2021).

Photo- and autoxidation of MUFAs and monounsaturated *n*-alken-1-ols yields mixtures of isomeric allylic hydroperoxyacids or hydroperoxyalcohols (Frankel, 1998; Rontani et al., 2012), respectively, which are converted to the corresponding hydroxyacids or diols after $NaBH_4$-reduction. The relative importance of photo- and autoxidation of these compounds can be readily calculated based on the proportion of *cis* isomers (which are produced specifically by autoxidation; Porter et al., 1995) and the temperature of seawater (Marchand and Rontani, 2001).

3. Results

3.1. Trophic environment across the Chukchi Sea transect

The main sterols: 24-norcholesta-5,22*E*-dien-3β-ol (24-norsterol), 27-nor-24-methylcholesta-5,22-dien-3β-ol, cholest-5-en-3β-ol (cholesterol), cholesta-5,22*E*-dien-3β-ol (22-dehydrocholesterol), cholesta-5,24-dien-3β-ol (desmosterol), 24-methylcholesta-5,22*E*-dien-3β-ol (*epi*-brassicasterol), 24-methylcholesta-5,24(28)-dien-3β-ol (24-methylenecholesterol), 24-ethylcholest-5-en-3β-ol (sitosterol) and 24(*E*)-ethylcholesta-5,24(28)-dien-3β-ol (fucosterol) were quantified across the transect to estimate the amount and nature of the algal material present in the SPM samples. The highest values of particulate sterol biomass were observed at stations 03, 02, 01, 09, 13 and 20, with a maximum at Station 03 suggesting the presence of a bloom event (Table 1, Fig. 4B). In contrast, the other stations, and notably the under ice station 26, contained relatively low concentrations of such sterols, indicating low phytoplankton abundances. For the majority of samples, sterol profiles were dominated by 24-norsterol, cholesterol, 22-dehydrocholesterol, *epi*-brassicasterol and 24-methylenecholesterol, the latter being particularly dominant at station 03. The proportion of sitosterol showed a marked increase at stations 21 and 22 (Fig. 4A).

Chl-*a*, fatty acid and phytol concentrations (Tables 2 and 3) confirmed the dominance of algal material at stations 03, 02, 01, 09, 13 and 20. The fatty acid profiles showed very low proportions of PUFAs (mainly $C_{16:4}$, $C_{18:4}$ and $C_{20:5}$) along the transect, reaching less than 4% of total fatty acids at station 03. SFAs were dominated by the classical $C_{14:0}$, $C_{16:0}$ and $C_{18:0}$, and MUFAs by $C_{16:1\Delta9}$ (palmitoleic acid), $C_{18:1\Delta9}$ (oleic acid) and $C_{18:1\Delta11}$ (vaccenic acid) (Table 2).

Long-chain saturated and monounsaturated primary alcohols (ranging from C_{14} to C_{22}) resulting from alkaline hydrolysis of zooplanktonic wax esters (Lee et al., 2006) were also detected, with highest concentrations at station 02 (Table 4). Interestingly, this station also exhibited the highest proportion of $C_{20:1}$ and $C_{22:1}$ *n*-alken-1-ols (Fig. 5A).

3.2. Biotic and abiotic degradation of phyto- and zooplanktonic lipids

3.2.1. Chlorophyll

Chlorophyll photooxidation estimates ranged from 33% to 96% along the transect (Table 3). Several biotic (dihydrophytol, phytanic, pristanic and 4,8,12-TMTD acids) and autoxidative (3,7,11,15-tetramethylhexadec-2(*Z/E*)-en-1,4-diols, 3,7,11,15-tetramethylhexadec-3(*Z/E*)-en-1,2-diols, and isophytol) degradation products of the chlorophyll phytyl side-chain could be detected in all samples (Fig. 6A). The phytyl side chain appeared to be strongly degraded at all stations except station 03, this degradation mainly involving autoxidative and biotic processes (Fig. 6B). The percentage of autoxidation products ranged from 4% to 29% of total isoprenoid compounds (Fig. 6B) and from 10% to 190% of the residual phytyl chain. Autoxidation was particularly intense at stations 01, 11, 14, 18, 20, 21 and 26. With the exception of station 03, biotic degradation products of phytol were dominant, ranging from 36% to 78% of total isoprenoid compounds.

3.2.2. MUFAs, n-alken-1-ols and sterols

Type II photosensitized oxidation of MUFAs appeared to be very limited except at station 01 where 24% of vaccenic acid was photooxidized (Fig. 7C). While palmitoleic acid was very weakly affected by autoxidative processes (Fig. 7A), autoxidation reached 73% and 64% in the case of oleic and vaccenic acids, respectively (Figs. 7B and 7C). Monounsaturated *n*-alken-1-ols arising from the hydrolysis of zooplanktonic wax esters were only weakly oxidized (Fig. 8). Interestingly, in the first part of the transect, photooxidation was more intense in the case of $C_{20:1\Delta11}$ and $C_{22:1\Delta11}$ *n*-alken-1-ols than for $C_{16:1\Delta9}$ and $C_{18:1\Delta9}$ (Fig. 8). Due to their relatively low contribution, photo- and autoxidation products of sterols (sum < 10%) were not quantified.

4. Discussion

4.1. Trophic environment at the different stations

Sterols possess structural characteristics (double bond positions, nuclear methylation and patterns of side-chain alkylation) restricted to a few groups of organisms (for reviews see Volkman, 1986; 2003; Rampen et al., 2010), and are often used to estimate phytoplanktonic diversity (Taipale et al., 2016). The diatom *Thalassiosira* aff. *antarctica* and the dinoflagellate *Gymnodinium simplex* have been proposed as potential sources of 24-norsterol (Rampen et al., 2007), which was found to be present in high proportion (ranging from 15 to 50%) along all the Chukchi Sea transect (Fig. 4A). Sterols that are methylated at the C-4 position including 4α,23,24-trimethyl-5α-cholest-22*E*-en-3-ol (dinosterol) are often employed as tracers for the contribution of dinoflagellates in the marine environment (Robinson et al., 1984). The absence (below detection limit) of such sterols at the different stations therefore allowed us to exclude a significant contribution of dinoflagellates across the transect. *T. antarctica*, which is found at high latitudes but not in tropical waters (Hasle and Heimdal, 1968), seems thus to strongly contribute to the phytoplankton community along all the Chukchi Sea transect. This centric diatom also contains a high proportion of 24-methylenecholesterol (Rampen et al., 2007), which is present with 24-norsterol at all stations (proportion ranging from 5 to 23% of total sterols) (Fig. 4A). It seems thus that *T. antarctica* or similar species belonging to the order of Thalassiosirales are one of the main phytoplankton contributors to these SPM samples. This assumption is in good agreement with the dominance of *T. antarctica* and *T. nordenskioeldii* previously observed in surface sediments of the Chukchi Sea (Asthakov et al., 2015). Further, *epi*-brassicasterol, which is also present in significant proportions along all the transect (Fig. 4A), suggests the presence of prymnesiophytes and notably of *Phaeocystis pouchetii*, whose sterol content comprises almost entirely this sterol (Nichols et al., 1991), and is widely

distributed in the Arctic (Riisgaard et al., 2015). The increasing proportions of sitosterol observed between stations 11 and 22 could potentially be attributed to the presence of increasing proportions of the diatoms *Asterionella glacialis*, *Haslea ostrearia* or *Amphiprora hyalina* (Volkman, 2003). Finally, the relatively high proportions of cholesterol present in most of the samples (Fig. 4A) suggest the occurrence of zooplanktonic material. Indeed, it is well-known that herbivorous and omnivorous crustaceans convert dietary phytosterols to cholesterol (Grieneisen, 1994; Behmer and Nes, 2003).

The presence of a high proportion of zooplanktonic material in the different samples is supported further by the detection of *n*-alkan-1-ols (Table 4) arising from alkaline hydrolysis of wax esters, which are generally the main storage lipids of marine zooplankton in high-latitude species (Lee et al., 2006). The most common *n*-alkan-1-ols of the wax esters of herbivorous copepods that undergo diapause (common in the Arctic) are $C_{20:1\Delta11}$ and $C_{22:1\Delta11}$, while omnivorous or carnivorous zooplankton generally show a predominance of $C_{14:0}$ and $C_{16:0}$ *n*-alkan-1-ols (Lee and Nevenzel, 1979; Albers et al., 1996). The proportion of herbivorous and omnivorous/carnivorous zooplankton was thus estimated on the basis of *n*-alkan-1-ol composition. The results obtained (Fig. 5B) show highest herbivorous zooplanktonic contribution at station 02 (where *Calanus glacialis* and *Eucalanus bungii* appeared to be dominant, Kim et al., 2020), which exhibits the highest concentration of *n*-alkan-1-ols (Table 4, Fig. 5A). Further, the very low amounts of the $C_{20:5}$ acid, a well-known component of numerous zooplankton species (Cass et al., 2014), suggests the presence of fecal pellets, where PUFAs are generally only present in low proportions (Harvey et al., 1987; Prahl et al., 1985) compared to zooplanktonic organisms. Fecal pellets generally settle out of the water column relatively quickly. Although coprophagy is usually the more important source of fecal pellet degradation (Iversen and Poulsen, 2007), they also experience fragmentation (coprorhexy)

leading to the formation of small slowly sinking particles (Smetacek, 1980), which could have been collected during the sampling.

The presence of PUFAs in only trace amounts is very surprising; indeed, these compounds are generally major components of high-altitude phytoplankton blooms (Parrish et al. 2005; Leu et al. 2006; Marmillot et al. 2020). We suggest that the relatively low proportions of PUFAs observed may be attributed to: (i) a highly detritic state of all the SPM samples investigated, (ii) a degradation of the more labile components of these samples (including PUFAs) between sampling and analysis (ca. 5 years) despite storage at -20 °C, or (iii) thermal losses during the treatment (see section 2.4). Although PUFAs appeared to be strongly degraded, the detection of residual amounts of the unusual fatty acids $C_{16:4}$ (synthesized by diatoms; Volkman, 2006) and $C_{18:4}$, a well-known acid component of copepod wax esters (Kattner, 1989; Graeve and Kattner, 1992), is in good agreement with the trophic environment described above. The $C_{18:4}$ fatty acid is also present in high proportion in *Phaeocystis* spp. (Sargent et al., 1985), but in this case it is accompanied by $C_{18:5}$ and $C_{22:6}$ fatty acids, which are absent in the SPM samples. The main source of the $C_{18:4}$ fatty acid in our SPM samples seems thus to be copepod wax esters.

4.2. Biotic and abiotic degradation of phyto- and zooplanktonic lipids

4.2.1. Chlorophyll

It was demonstrated recently that high solar irradiances favour photobleaching of chlorophyll (sensitizer) at the expense of Type-II (i.e. involving singlet oxygen) photosensitized oxidation of lipids (the photodynamic effect) (Amiraux et al., 2016; Rontani et al., 2021). Since the SPM samples investigated in the present work were collected near to the surface (5 m), thereby receiving highest solar irradiance (up to 500 W m^{-2}, Dr. Ha, unpublished results), the elevated

CPPI-based chlorophyll photodegradation estimates are not surprising (Table 3). Further, we note that even at station 03, 45% of chlorophyll was photooxidized, suggesting the diatoms were in a poor physiological state, despite an apparent bloom event.

Isoprenoid compounds resulting from the degradation of the chlorophyll phytyl side-chain were not only useful for quantifying chlorophyll photodegradation (see section 2.7), but also for identifying the importance of autoxidative and biotic alteration of primary production. Autoxidation of the phytyl chain affords mainly isophytol (Rontani and Galeron, 2016), 3,7,11,15-tetramethylhexadec-2(*Z/E*)-en-1,4-diols and 3,7,11,15-tetramethylhexadec-3(*Z/E*)-en-1,2-diols (Rontani and Aubert, 2005) (Fig. 9), which are specific tracers of these degradative processes. The detection of significant proportions of these compounds in some SPM samples (Fig. 6) thus demonstrates the important role played by autoxidation in the degradation of primary producers.

Pelagic crustaceans assimilate the chlorophyll phytyl chain when feeding herbivorously (Prahl et al., 1984; Harvey et al., 1987). During this metabolism, phytol is successively hydrogenated to dihydrophytol, oxidized to phytanic acid, and then cleaved to pristanic and 4,8,12-TMTD acids by way of classical α- and β-oxidation sequences (Fig. 9) (for a review see Rontani and Volkman, 2003). Such isoprenoid compounds have been detected previously in different *Calanus* species (Avigan and Blumer, 1968; Prahl et al., 1984). As such, while phytol logically dominates isoprenoid compounds at station 03 due to a declining bloom event mainly composed of weakly altered diatoms, the other stations exhibit a strong dominance of phytanic and pristanic acids (Fig. 6B), which confirms a strong contribution of zooplanktonic material.

4.2.2. Unsaturated fatty acids

Photodegradation rates of unsaturated fatty acids increases, logically, with their degree of unsaturation (Frankel, 1998), such that PUFAs are very reactive towards Type-II

photosensitized oxidation processes (Frankel, 1998; Rontani et al., 1998). Unfortunately, the resulting oxidation products cannot be used as quantitative tracers of Type-II photooxidation processes in the environment due to the instability of the primary oxidation products formed (Rontani and Belt, 2020). However, it was demonstrated previously that PUFAs are photodegraded approximately 5 times faster than MUFAs in dead cells of diatoms (Rontani et al., 2011). Based on the very weak photooxidation percentage of MUFAs in our SPM samples (Fig. 7; mean value 1.9 ± 4.2%), the contribution of Type-II photosensitized oxidation processes to the degradation of PUFAs thus appeared to be very weak (~ 10%). This very weak photooxidative alteration of PUFAs and MUFAs results likely from the limitation of the photodynamic effect under high solar irradiances (Amiraux et al., 2016; Rontani et al., 2021).

Whereas autoxidation of palmitoleic acid was limited to 25% in SPM samples (Fig. 7A), it reached 73% in the case of oleic acid (Fig. 7B). These differences of reactivity may be attributed to the origins of these MUFAs. Indeed, although palmitoleic and oleic acids are not unambiguous biomarkers of phytoplankton and zooplankton inputs (Wakeham and Canuel, 1988), they are often used to obtain relative indication of the predominance of algal vs. zooplanktonic sources (Tolosa et al., 2004). Palmitoleic acid, which is a major fatty acid of diatoms (Volkman et al., 1989; Dunstan et al., 1993), is also present in several bacteria (e.g., de Carvalho and Caramujo, 2014), and may be found in high proportion in storage lipids of zooplankton feeding on diatoms (Lee et al., 2006). In contrast, omnivorous and carnivorous zooplankton species are characterized by wax esters with high amounts of oleic acid (Lee et al., 2006). However, we note that *Phaeocystis* spp. may also contain elevated levels of oleic acid (Dalsgaard et al., 2003). On the basis of high proportions of phytanic and pristanic acids observed in all SPM samples (Fig. 5), we consider that the major source of oleic acid to be omnivorous zooplankton (more precisely euphausiids or *Metridia pacifica* detected in the samples analysed, Kim et al., 2020) rather than prymnesiophytes. Autoxidation seems thus to

be stronger in faecal pellets of omnivorous and carnivorous zooplankton than in diatoms or herbivorous zooplankton feeding on diatoms. Further, we note that the highest autoxidation percentages of oleic acid were observed at stations 01, 11, 14, 18, 20, 21 and 26, which also exhibit the highest autoxidation of the chlorophyll phytyl side-chain (Fig. 6B).

Based on: (i) pseudo-first order autoxidative degradation rates of palmitoleic and $C_{20:5}$ acids previously measured during incubation of dead diatom cells (1.5×10^{-3} and 2.7×10^{-2} h^{-1}, respectively; Rontani et al., 2014), and (ii) the mean autoxidation percentage (14.4 ± 7.7%) of palmitoleic acid observed in the different SPM samples (Fig. 6A), an important contribution of autoxidation to the disappearance of PUFAs in these samples may be expected. However, it is well known that PUFAs are also significantly reduced relative to total fatty acids during passage through the gut of copepods (Harvey et al., 1987; Prahl et al., 2009). Consequently, due to the important contribution of zooplanktonic faecal pellets to the SPM samples analysed, an important degradation of PUFAs during copepod grazing is very likely. Note that a significant degradation during the storage and the treatment cannot be totally excluded.

Surprisingly, vaccenic acid, well-known to be specific to bacteria (Lambert and Moss, 1983; Sicre et al., 1988), also appeared to be strongly autoxidized (Fig. 7C). Autoxidation states of vaccenic and oleic acids are not significantly different (Kruskal-Wallis, n=26 $p = 0.817 > 0.05$), while the autoxidation state of vaccenic acid is significantly different to that of palmitoleic acid (Kruskal-Wallis, n=26 $p = 0.00025 < 0.05$). Autoxidation of vaccenic acid seems thus to mainly intervene in omnivorous or carnivorous zooplanktonic faecal pellets, rather than in heterotrophic bacteria associated to diatom phytodetritus or present in faecal pellets of herbivorous zooplankton feeding on diatoms. Interestingly, the lipid composition of bacterivorous ciliates resembles that of their prey (Harvey et al., 1987; Boëchat and Adrian, 2005). Recently, the presence of high proportions of *trans* MUFAs in SPM samples collected under sea ice in Baffin Bay was attributed to the ingestion of bacteria stressed by salinity in

internal brines of sea ice by sympagic ciliates, and the direct incorporation of these highly isomerized dietary fatty acids (Burot et al., 2021). A trophic link between copepods and ciliates has been well established (Pierce and Turner 1992), and some authors have shown that lipids of bacterial origin can be transferred up the food web without modification to copepods that consume bacterivorous ciliates (Ederington et al., 1995). The presence of both vaccenic and oleic acids in copepod wax esters, as in the case of some euphausiids (Lee et al., 2006), could thus explain their similar autoxidative reactivity (Figs. 7B and 7C).

4.2.3. Monounsaturated n-alkan-1-ols

Although Type II photosensitized oxidation of monounsaturated *n*-alkan-1-ols was also relatively weak (Fig. 8), likely due to the strong chlorophyll photobleaching, it is interesting to note that $C_{20:1\Delta11}$ and $C_{22:1\Delta11}$ *n*-alkan-1-ols (specific to herbivorous copepod wax esters; Lee et al., 2006) were more photooxidized in the first five stations (01, 02, 03, 09, and 11) than the non-specific $C_{16:1\Delta9}$ and $C_{18:1\Delta9}$ *n*-alken-1-ols (Kruskal-Wallis, n=20 $p = 0.00516 < 0.05$). Previously, a strong photooxidation of $C_{20:1\Delta11}$ and $C_{22:1\Delta11}$ *n*-alken-1-ols was observed in sinking particles collected in summer at 100 m in the Beaufort Sea (Rontani et al., 2012), and attributed to a very high efficiency of Type-II photosensitized oxidation processes in faecal pellets of herbivorous copepods. A very efficient transfer of singlet oxygen from more or less digested diatoms to the wax esters present in the lipid droplets trapped in faecal pellets (Najdek et al., 1994) was also proposed. The strongest photooxidation observed in the Beaufort Sea likely results from a fast transfer of faecal pellets to deep waters where the intensity of solar irradiance should be sufficiently weak to favour the photodynamic effect at the expense of chlorophyll photobleaching. The weak and selective photooxidation of $C_{20:1\Delta11}$ and $C_{22:1\Delta11}$ *n*-alken-1-ols observed during the present study confirms: (i) the involvement of this process in faecal pellets of herbivorous copepods, and (ii) the key role played by solar irradiance and

sinking rates in the efficiency of the photodynamic processes. Due to the intensity of solar irradiance during summers, only the chlorophyll of senescent diatom cells and the debris of herbivorous zooplankton faecal pellets (which are suspended in surface waters of the Chukchi Sea), is thus strongly affected by photooxidation processes.

Monounsaturated *n*-alkan-1-ols also appeared to be weakly affected by autoxidative processes in our Chukchi Sea samples (Fig. 8). Since autoxidation of monounsaturated long-chain MUFAs and *n*-alkan-1-ols involves attack of the allylic positions of their isolated double bonds (Frankel, 1998), their degradation rates should be very similar and only weakly impacted by esterification. The differences in reactivity observed between these alcohols and oleic and vaccenic acids (Figs. 7B and 7C) are thus very surprising. Autoxidation of wax esters of omnivorous or carnivorous copepods containing high amounts of oleic acid and of the unreactive $C_{14:0}$ and $C_{16:0}$ alcohols (Albers et al., 1996) seems thus to be strongly favoured (Fig. 7B), while wax esters of herbivorous copepods dominated by $C_{20:1\Delta11}$ and $C_{22:1\Delta11}$ *n*-alken-1-ols and $C_{14:0}$, $C_{16:0}$, $C_{20:1}$ and $C_{22:1}$ fatty acids (Lee et al., 2006) are only weakly affected (Fig. 8). It was previously observed that herbivorous amphipods are somewhat resistant to oxidative stress due to the presence of high concentrations of antioxidants (i.e. mycosporine-like amino acids and carotenoids) ingested from their algal diet (Abele and Puntarulo, 2004; Obermüller et al., 2005; Obermüller, 2006), while carnivorous species are very sensitive to this stress due to their lower accumulation of algal antioxidants via the food chain (Obermüller et al., 2005). The differences in autoxidative reactivity observed in the present work between oleic acid (main acid counterpart of omnivorous or carnivorous copepod wax esters; Albers et al., 1996) and $C_{20:1\Delta11}$ and $C_{22:1\Delta11}$ *n*-alken-1-ols (main alcohol counterparts of herbivorous copepod wax esters; Lee et al., 2006) thus complement these previous findings.

It is generally considered that sinking of zooplanktonic faecal pellets to the seafloor is strongly limited by coprophagy (Paffenhöfer and Knowles, 1979) and bacterial decomposition

(Smetacek, 1985). In the case of faecal pellets of carnivorous or omnivorous zooplankton, autoxidation processes seem thus to also contribute to their degradation.

4. Conclusions

Analysis of the lipid content of SPM samples collected in surface waters of the Chukchi Sea enabled us to confirm: (i) their detritic character, (ii) the dominance of diatoms (Thalassiosirales) among primary producers, and (iii) the presence of high proportions of zooplanktonic (copepods) faecal pellet debris during the summer period. Type II photosensitized oxidation of phyto- and zooplanktonic lipids (photodynamic effect) appeared to be relatively limited, likely due to the enhancement of photobleaching of chlorophyll (sensitizer) by the high solar irradiance observed near to the surface. The weak photooxidation of zooplanktonic wax esters observed in these SPM samples contrasts with the strong photooxidative alteration of these compounds previously observed in sinking particles collected from the Beaufort Sea in summer (Rontani et al., 2012). The photodynamic effect seems thus to be favoured in large faecal pellets of herbivorous copepods sinking quickly in weakly irradiated zones. In contrast, autoxidative processes, which can operate in all oxic aquatic environments (Schaich, 2005) and potentially affect all unsaturated lipids (Rontani, 2012; Rontani and Belt, 2020), acted more intensively in faecal pellets of omnivorous or carnivorous copepods than in those of herbivorous counterparts. Such differences of reactivity were attributed to the consumption of algal antioxidants during the diet of omnivorous or carnivorous copepods, which should favour the establishment of free radical oxidation processes.

Acknowledgements

This research was a part of the project titled ‘Korea-Arctic Ocean Warming and Response of Ecosystem (K-AWARE, KOPRI, 1525011760)’, funded by the Ministry of Oceans and

Fisheries, Korea. Thanks are due to the Feder Oceanomed (No. 1166-39417) for the funding of the GC-QTOF employed and to two anonymous reviewers for their useful and constructive comments.

References

Abe, Y., Matsuno, K., Fujiwara, A., Yamaguchi, A., 2020. Review of spatial and inter-annual changes in the zooplankton community structure in the western Arctic Ocean during summers of 2008–2017. Progress in Oceanography 186, 102391.

Abele, D., Puntarulo, S., 2004. Formation of reactive species and induction of antioxidant defence systems in polar and temperate marine invertebrates and fish. Comparative Biochemistry and Physiology Part A: Molecular and Integrative Physiology 138, 405-415.

Afi, L., Metzger, P., Largeau, C., Connan, J., Berkaloff, C., Rousseau, B., 1996. Bacterial degradation of green macroalgae: incubation of *Chlorella emersonii* and *Chlorella vulgaris* with *Pseudomonas oleovorans* and *Flavobacterium aquatile*. Organic Geochemistry 25, 117-130.

Albers, C.S., Kattner, G., Hagen W., 1996. The compositions of wax esters, triacylglycerols and phospholipids in Arctic and Antarctic copepods: evidence of energetic adaptations. Marine Chemistry 55, 347-358.

Amiraux, R., Jeanthon, C., Vaultier, F., Rontani, J.-F., 2016. Paradoxical effects of temperature and solar irradiance on the photodegradation state of killed phytoplankton. Journal of Phycology 52, 475-485.

Arrigo, K.R., van Dijken, G. L., 2015. Continued increases in Arctic Ocean primary production. Progress in Oceanography 136, 60–70.

Astakhov, A.S., Bosin, A.A. Kolesnik A.N., Obrezkova, M.S., 2015. Sediment geochemistry and diatom distribution in the Chukchi Sea. Oceanography 28, 190-201.

Avigan, J., Blumer, M., 1968. On the origin of pristane in marine organisms. Journal of Lipid Research 9, 350-352.

Bates, N.R., 2006. Air-sea CO_2 fluxes and the continental shelf pump of carbon in the Chukchi Sea adjacent to the Arctic Ocean. Journal of Geophysical Research 111, C10013.

Behmer, S.T., Nes, W.D. 2003. Insect sterol nutrition and physiology: a global overview. Advances in Insect Physiology 31, 1-72.

Boëchat, I.G., Adrian, R., 2005. Biochemical composition of algivorous freshwater ciliates: You are not what you eat. FEMS Microbiology Ecology 53, 393-400.

Burot, C., Amiraux, R., Bonin, P., Guasco, S., Babin, M., Joux, F., Marie D., Vilgrain, L., Heipieper, H., Rontani, J.-F., 2021. Viability and stress state of bacteria associated with primary production or zooplankton-derived suspended particulate matter in summer along a transect in Baffin Bay (Arctic Ocean). Science of the Total Environment 770, 145252.

Cason, J., Graham, D.W., 1965. Isolation of isoprenoid acids from a California petroleum. Tetrahedron 21, 471-483.

Cass, C.J., Daly, K.L., Wakeham, S.G., 2014. Assessment of storage lipid accumulation patterns in eucalanoid copepods from the eastern tropical Pacific Ocean. Deep Sea Research I 93, 117-130.

Chen, C.-T. A., Borges, A.V., 2009. Reconciling opposing views on carbon cycling in the coastal ocean: Continental shelves as sinks and near-shore ecosystems as sources of atmospheric CO_2. Deep Sea Research II 56, 578-590.

Christodoulou, S., Marty, J.-C., Miquel, J.-C., Volkman, J.K., Rontani, J.-F., 2009. Use of lipids and their degradation products as biomarkers for carbon cycling in the northwestern Mediterranean Sea. Marine Chemistry 113, 25-40.

Christodoulou S., Joux F., Marty J.-C., Sempéré R., Rontani J.-F., 2010. Comparative study of UV and visible light induced degradation of lipids in non-axenic senescent cells of *Emiliania huxleyi*. Marine Chemistry 119, 139-152.

Comiso, J.C., Parkinson, C.L., Gersten, R., Stock, L., 2008. Accelerated decline in the Arctic sea ice cover. Geophysical Research Letters 35, L01703.

Cuny, P., Rontani, J.-F., 1999. On the widespread occurrence of 3-methylidene-7,11,15-trimethylhexadecan-1,2-diol in the marine environment: a specific isoprenoid marker of chlorophyll photodegradation. Marine Chemistry 65, 155-165.

Cuny, P., Romano, J.-C., Beker, B., Rontani, J.-F., 1999. Comparison of the photodegradation rates of chlorophyll chlorin ring and phytol side chain in phytodetritus: is the phytyldiol versus phytol ratio (CPPI) a new biogeochemical index? Journal of the Experimental and Marine Biology and Ecology 237, 271–290.

Dalsgaard, J., St. John, M., Kattner, G., Müller-Navarra, D., Hagen, W., 2003. Fatty acid trophic markers in the pelagic marine environment. Advances in Marine Biology 46, 225-340.

Dunstan, G.A., Volkman, J.K., Barrett, S.M., Leroi, J.-M., Jeffrey, S.W., 1993. Essential polyunsaturated fatty acids from 14 species of diatom (Bacillariophyceae). Phytochemistry 35, 155-161.

Ederington, M.C., McManus, G.B., Harvey, H.R., 1995. Trophic transfer of fatty acids, sterols, and a triterpenoid alcohol between bacteria, a ciliate, and the copepod *Acartia tonsa*. Limnology and Oceanography 40, 860-867.

Frankel, E.N., 1998. Lipid oxidation. The Oily Press, Dundee.

Graeve, M., Kattner, G., 1992. Species-specific differences in intact wax esters of *Calanus hyperboreus* and *C. finmarchicus* from Fram Strait — Greenland Sea. Marine Chemistry 39, 269-281.

Grebmeier, J.M., McRoy, C.P., Feder, H.M., 1988. Pelagic-benthic coupling on the shelf of the northern Bering and Chukchi Seas. I. Food supply source and benthic biomass. Marine Ecology Progress Series 48, 57-67.

Grebmeier, J.M., Cooper, L.W., Feder, H.M., Sirenko, B.I., 2006. Ecosystem dynamics of the Pacific-influenced Northern Bering and Chukchi Seas in the Amerasian Arctic. Progress in Oceanography 71, 331-361.

Grieneisen, M.L., 1994. Recent advances in our knowledge of ecdysteroid biosynthesis in insects and crustaceans. Insect Biochemistry and Molecular Biology 24, 115-132.

Harvey, H.R., Eglinton, G., O'hara, S.C.M., Corner, E.D.S., 1987. Biotransformation and assimilation of dietary lipids by *Calanus* feeding on a dinoflagellate. Geochimica et Cosmochimica Acta 51, 3031–3040.

Hasle, G.R., Heimdal, B.R., 1968. Morphology and distribution of the marine centric diatom *Thalassiosira antarctica* Comber. Journal of the Royal Microscopical Society 88, 357-369.

Hunt Jr., G.L., Blanchard, A.L., Boveng P., Dalpadado, P., Drinkwater, K.F., Eisner, L., Hopcroft, R.R., Kovacs, K.M., Norcross, B.L, Renaud, P., Reigstad, M., Renner, M., Rune Skjoldal, H., Whitehouse, A., Woodgate, R.A., 2013. The Barents and Chukchi Seas: Comparison of two Arctic shelf ecosystems. Journal of Marine Systems 109–110, 43-68.

IPCC (2013) Climate change 2013: Impact, adaptation and vulnerability. Contribution of working group I to the Fifth Assessment Report of the Intergovernmental Panel on Climate Change. Cambridge University Press, Cambridge.

Iversen, M.H., Poulsen, L. K., 2007. Coprorhexy, coprophagy, and coprochaly in the copepods *Calanus helgolandicus, Pseudocalanus elongatus*, and *Oithona similis*. Marine Ecology Progress Series 350, 79-89.

Kattner, G., 1989. Lipid composition of *Calanus finmarchicus* from the North Sea and the arctic. A comparative study. Comparative Biochemistry and Physiology Part B 94, 185-188.

Kim, B.K., Jung, J., Lee, Y., Cho, K.-H., Gal, J.-K., Kang, S.-H., Ha, S.-Y., 2020. Characteristics of the biochemical composition and bioavailability of phytoplankton-derived particulate organic matter in the Chukchi Sea, Arctic. Water 12, 2355.

Kitamura, M., Amakasu, K. Kikuchi, T., Nishino, S., 2017. Seasonal dynamics of zooplankton in the southern Chukchi Sea revealed from acoustic backscattering strength. Continental Shelf Research 133, 47-58.

Korytowski, W., Bachowski, G.J., Girotti, A.W., 1992. Photoperoxidation of cholesterol in homogeneous solution, isolated membranes, and cells: comparison of the 5α- and 6β-hydroperoxides as indicators of singlet oxygen intermediacy. Photochemistry and Photobiology 56, 1-8.

Kulig, M.J., Smith, L.L., 1973. Sterol metabolism. XXV. Cholesterol oxidation by singlet molecular oxygen. Journal of Organic Chemistry 38, 3639-3642.

Lambert, M.A., Moss, C.W., 1983. Comparison of the effects of acid and base hydrolyses on hydroxy and cyclopropane fatty acids in bacteria. Journal of Clinical Microbiology 18, 1370-1377.

Lee, R.F., Hagen, W., Kattner, G., 2006. Lipid storage in marine zooplankton. Marine Ecology Progress Series 307, 273-306.

Lee, R.F., Nevenzel, J.C., 1979. Wax esters in the marine environment: origin and composition of the wax from Bute Inlet, British Columbia. Journal of the Fisheries Research Board of Canada 36, 1519-23.

Leu, E., Falk-Petersen, S., Kwasniewski, S., Wulff, A., Edvardsen, K., O. Hessen, D., 2006. Fatty acid dynamics during the spring bloom in a high Arctic fjord: importance of abiotic factors versus community changes. Canadian Journal of Fisheries and Aquatic Sciences 63, 2760–2779.

Leu, E., Søreide, J.E., Hessen, D.O., Falk-Petersen, S., Berge, J., 2011. Consequences of changing sea-ice cover for primary and secondary producers in the European Arctic shelf seas: Timing, quantity, and quality. Progress in Oceanography 90, 18–32.

Loidl-Stahlhofen, A., Hannemann, K., Spiteller, G., 1994. Generation of α-hydroxyaldehydic compounds in the course of lipid peroxidation. Biochimica et Biophysica Acta - Lipids and Lipid Metabolism 1213, 140-148.

Mäkinen, K., Elfving, M., Hänninen, J., Laaksonen, L., Rajasilta, M., Vuorinen, I., Suomela, J.-P., 2017. Fatty acid composition and lipid content in the copepod *Limnocalanus macrurus* during summer in the southern Bothnian Sea. Helgoland Marine Research 71, 11.

Marchand, D., Rontani, J.-F., 2001. Characterisation of photooxidation and autoxidation products of phytoplanktonic monounsaturated fatty acids in marine particulate matter and recent sediments. Organic Geochemistry 32, 287-304.

Marmillot, V., Parrish, C.C., Tremblay, J.-E., Gosselin, M., MacKinnon, J.F., 2020. Environmental and biological determinants of algal lipids in Western Arctic and subarctic seas. Frontiers in Environmental Science 8, 538635.

Morrissey, P.A., Kiely, M., 2006. Oxysterols: formation and biological function. In. Advanced Dairy Chemistry 3rd edition, Vol. 2, Lipids, Fox. P.F., McSweeney, P.L.H. (Eds.), Springer, New-York, pp. 641-674.

Najdek, M., Puškarić, S., Bochdansky, A.B., 1994. Contribution of zooplankton lipids to the flux of organic matter in the northern Adriatic Sea. Marine Ecology Progress Series 111, 241-249.

Nichols, P.D., Skerratt, J.H., Davidson, A., Burton, H., McMeekin, T.A., 1991. Lipids of cultured *Phaeocystis pouchetii*: Signatures for food-web, biogeochemical and environmental studies in Antarctica and the Southern ocean. Phytochemistry 30, 3209-3014.

Obermüller, B., Karsten, U., Abele, D., 2005. Response of oxidative stress parameters and sunscreening compounds in Arctic amphipods during experimental exposure to maximal natural UVB radiation. Journal of Experimental Marine Biology and Ecology 323, 100-117.

Obermüller, B., 2006. Effects of UV-radiation on crustaceans from polar and temperate coastal ecosystems. PhD thesis. Universität Bremen, Deutschland.

Onarheim, I.H., Eldevik, T., Smedsrud, L., Stroeve, J.C., 2018. Seasonal and regional manifestation of Arctic sea ice loss. Journal of Climate, 31, 4917-4932.

Paffenhöfer, G., Knowles, S.C., 1979. Ecological implications of fecal pellet size, production and consumption by copepods. Journal of Marine Research 37, 35-49.

Parrish, C.C., Thompson, R.J., Deibel, D., 2005. Lipid classes and fatty acids in plankton and settling matter during the spring bloom in a cold ocean coastal environment. Marine Ecology Progress Series 286, 57–68.

Parsons, T.R., Maita, Y., Lalli, C.M.,1984. A manual of chemical and biological methods for seawater analysis. Oxford, Pergamon Press, 173 pp.

Piepenburg, D., 2005. Recent research on Arctic benthos: common notions need to be revised. Polar Biology 28, 733–755.Pierce, R.W., Turner, J.T., 1992. Ecology of planktonic ciliates in marine food webs. Reviews in Aquatic Sciences 6, 139-181.

Porter, N.A., Caldwell, S.E., Mills, K.A., 1995. Mechanisms of free radical oxidation of unsaturated lipids. Lipids 30, 277-290.

Post, E., Bhatt, U. S., Bitz, C. M., Brodie, J. F., Fulton, T. L., Hebblewhite, M., Kerby, J., Kutz, S.J., Stirling, I., Walker, D.A., 2013. Ecological consequences of sea-ice decline. Science 341(6145), 519–524.

Prahl, F.G., Eglinton, G., Corner, E.D.S., O'Hara, S.C.M., Forsberg, T.E.V., 1984. Changes in plant lipids during passage through the gut of *Calanus*. Journal of the Marine Biological Association of the United Kingdom 64, 317-333.

Prahl, F.G., Eglinton, G., Corner, E.D.S., O'Hara, S.C.M., 1985. Faecal lipids released by fish feeding on zooplankton. Journal of the Marine Biological Association of the United Kingdom 65, 547-560.

Rampen, S.W., Schouten, S., Abbas, B., Elda Panoto, F., Muyzer, G., Campbell, C.N., Fehling, J., Sinninghe Damsté, J.S., 2007. On the origin of 24-norcholestanes and their use as age-diagnostic biomarkers. Geology 35, 419-422.

Rampen, S.W., Abbas, B.A., Schouten, S., Sinninghe-Damsté, J.S.S., 2010. A comprehensive study of sterols in marine diatoms (Bacillariophyta): Implications for their use as tracers for diatom productivity. Limnology and Oceanography 55, 91-105.

Renaut, S., Devred, E., Babin, M., 2018. Northward expansion and intensification of phytoplankton growth during the early ice-free season in Arctic. Geophysical Research Letters 45, 10590–10958.

Riisgaard, K., Nielsen, T.G., Hansen, P.J., 2015. Impact of elevated pH on succession in the Arctic spring bloom. Marine Ecology Progress Series 530, 63-75.

Robinson, N., Eglinton, G., Brassell, S.C., Cranwell, P.A., 1984. Dinoflagellate origin for sedimentary 4α-methylsteroids and 5α(H)-stanols. Nature 308, 439–442.

Rontani, J.-F., Baillet, G., Aubert, C., 1991. Production of acyclic isoprenoid compounds during the photodegradation of chlorophyll in seawater. Journal of Photochemistry and Photobiology A59, 369–377.

Rontani, J.-F., Grossi, V., Faure, F., Aubert, C., 1994. ''Bound'' 3-methylidene-7,11,15-trimethylhexadecan-1,2-diol: a new isoprenoid marker for the photodegradation of chlorophyll-a in seawater. Organic Geochemistry 21, 135-142.

Rontani, J.-F., Cuny, P., Grossi, V., 1998. Identification of a pool of lipid photoproducts in senescent phytoplanktonic cells. Organic Geochemistry 29, 1215-1225.

Rontani, J.-F., Volkman, J.K., 2003. Phytol degradation products as biogeochemical tracers in aquatic environments. Organic Geochemistry 34, 1-35.

Rontani, J.-F., Rabourdin, A., Marchand, D., Aubert, C., 2003. Photochemical oxidation and autoxidation of chlorophyll phytyl side chain in senescent phytoplanktonic cells: potential sources of several acyclic isoprenoid compounds in the marine environment. Lipids 38, 241-253.

Rontani, J.-F., Aubert, C., 2005. Characterization of isomeric allylic diols resulting from chlorophyll phytyl side chain photo- and autoxidation by electron ionization gas chromatography/mass spectrometry. Rapid Communications in Mass Spectrometry 19, 637-646.

Rontani, J.-F., Belt, S.T., Vaultier, F., Brown, T.A., 2011. Visible light-induced photo-oxidation of highly branched isoprenoid (HBI) alkenes: a significant dependence on the number and nature of the double bonds. Organic Geochemistry 42, 812-822.

Rontani, J.-F., 2012. Photo- and free radical-mediated oxidation of lipid components during the senescence of phototrophic organisms. In: T. Nagata Ed., Senescence. Intech, Rijeka, pp. 3-31.

Rontani, J.-F., Charriere, B., Forest, A., Heussner, S., Vaultier, F., Petit, M., Delsaut, N., Fortier, L., Sempéré, R., 2012. Intense photooxidative degradation of planktonic and bacterial lipids in sinking particles collected with sediment traps across the Canadian Beaufort Shelf (Arctic Ocean). Biogeosciences 9, 4787-4802.

Rontani, J.-F., Belt, S., Vaultier, F., Brown, T., Massé, G., 2014. Autoxidative and photooxidative reactivity of highly branched isoprenoid (HBI) alkenes. Lipids, 49(5), 481-494.

Rontani, J.-F., Galeron, M.-A., 2016. Autoxidation of chlorophyll phytyl side-chain in senescent phototrophic organisms: a potential source of isophytol in the environment. Organic Geochemistry 97, 37-40.

Rontani, J.-F., Belt, S.T., 2020. Photo- and autoxidation of unsaturated algal lipids in the marine environment: An overview of processes, their potential tracers, and limitations. Organic Geochemistry 139, 103941.

Rontani, J.-F., Amiraux, R., Smik, L., Wakeham, S.G., Paulmier, A., Vaultier, F., Sun-Yong, H., Jun-oh, M., Belt, S.T., 2021. Type II photosensitized oxidation in senescent microalgal cells at different latitudes: Does low under-ice irradiance in polar regions enhance efficiency? Science of The Total Environment 779, 146363.

Sargent, J.R., Eilertsen, H.C., Falk-Petersen, S., Taasen, J.P., 1985. Carbon assimilation and lipid production in phytoplankton in northern Norwegian fjords. Marine Biology 85, 109-116.

Schaich, K.M., 2005. Lipid oxidation: theoretical aspects. In: Shahidi, F. (Ed.), Bailey's Industrial Oil and Fat Products. John Wiley & Sons, Chichester, pp. 269-355.

Serreze, M. C., Holland, M. M., Stroeve, J., 2007. Perspectives on the Arctic's shrinking sea-ice cover. Science 315, 1533–1536.

Sicre, M.-A., Paillasseur, J.-L., Marty, J.-C., Saliot, A., 1988. Characterization of seawater samples using chemometric methods applied to biomarker fatty acids. Organic Geochemistry 12, 281-8.

Smetacek, V.S., 1980. Zooplankton standing stock, copepod faecal pellets and particulate detritus in Kiel Bight. Estuarine and Coastal Marine Science 11, 477-490.

Smetacek, V.S., 1985. Role of sinking in diatom life-history cycles: ecological, evolutionary and geological significance. Marine Biology 84, 239-251.

Smith, L.L., 1981. The Autoxidation of Cholesterol. Plenum Press, New York.

Springer, A.M., McRoy, C.P., 1993. The paradox of pelagic food webs in the northern Bering Sea—III. Patterns of primary production. Continental Shelf Research 13, 575-599.

Sun, M.-Y., Aller, R.C., Lee, C., Wakeham, S.G., 1999. Enhanced degradation of algal lipids by benthic macrofaunal activity: Effect of *Yoldia limatula*. Journal of Marine Research 57, 775-804.

Taipale, S. J., Hiltunen, M., Vuorio, K., Peltomaa, E., 2016. Suitability of phytosterols alongside fatty acids as chemotaxonomic biomarkers for phytoplankton. Frontiers in Plant Science 7, 212.

Tolosa, I., Vescovali, I., Leblond, N., Marty, J.-C., de Mora, S., Prieur, L., 2004. Distribution of pigments and fatty acid biomarkers in particulate matter from the frontal structure of the Alboran Sea (SW Mediterranean Sea). Marine Chemistry 88, 103-125.

Volkman, J.K., 1986. A review of sterol markers for marine and terrigenous organic matter. Organic Geochemistry 9, 83-99.

Volkman, J.K., Jeffrey, S.W., Nichols, P.D., Rogers, G.I., Garland, C.D., 1989. Fatty acid and lipid composition of 10 species of microalgae used in mariculture. Journal of Experimental Marine Biology and Ecology 128, 219-240.

Volkman, J.K., Barrett, S.M., Blackburn, S.I., Mansour, M.P., Sikes, E.L., Gelin, F., 1998. Microalgal biomarkers: a review of recent research developments. Organic Geochemistry 29, 1163-1179.

Volkman, J.K., 2003. Sterols in microorganisms. Applied Microbiology and Biotechnology 60, 495-506.

Volkman, J.K., 2006. Lipid Markers for Marine Organic Matter. In: Volkman, J.K. (Ed.) Marine Organic Matter: Biomarkers, Isotopes and DNA. The Handbook of Environmental Chemistry. Springer, Berlin, Heidelberg. vol 2N. pp 27-70.

Wakeham, S.G., Canuel, E., 1988. Organic geochemistry of particulate matter in the eastern tropical North Pacific Ocean: Implications for particle dynamics. Journal of Marine Research 46, 183-213.

Wassmann, P., Carroll, J., Bellerby, R.G.J., 2008. Carbon flux and ecosystem feedback in the northern Barents Sea in an era of climate change: An introduction. Deep Sea Research Part II 55, 2143–2153.

FIGURE CAPTIONS

Figure 1. Map of the study area with location of the stations investigated in Chukchi Sea. The line corresponds to the limit of ice at the time of sampling.

Figure 2. GC-QTOF determination of the double bond position of MUFAs with the TMS derivatives of their oxidation products in the SPM sample collected at station 02.

Figure 3. GC-QTOF determination of the double bond position of monounsaturated *n*-alkan-1-ols with the TMS derivatives of their oxidation products in the SPM sample collected at station 02.

Figure 4. Relative proportions (A) and concentrations (ng L^{-1}) (B) of sterols in SPM samples collected at the different stations investigated.

Figure 5. Concentrations (µg L^{-1}) of *n*-alkan-1-ols (A) and proportions of herbivorous and omnivorous or carnivorous zooplankton (B) in SPM samples collected at the different stations investigated.

Figure 6. Concentrations (ng L^{-1}) of chlorophyll phytyl side-chain and its main degradation products (A) and estimates of the proportion of its biotic, autoxidative and photooxidative degradation (B) in SPM samples collected at the different stations investigated.

Figure 7. Relative percentage of intact, autoxidized and photooxidized palmitoleic (A), oleic (B) and vaccenic (C) acids in SPM samples collected at the different stations investigated.

Figure 8. Relative percentage of intact, autoxidized and photooxidized $C_{16:1\Delta9}$, $C_{18:1\Delta9}$, $C_{20:1\Delta11}$ and $C_{22:1\Delta11}$ *n*-alkan-1-ols in SPM samples collected at the different stations investigated.

Figure 9. Biotic and abiotic degradation of the chlorophyll phytyl side-chain (compounds in blue were quantified during the present work).

Figure

Click here to access/download;Figure;Figure 1.pdf

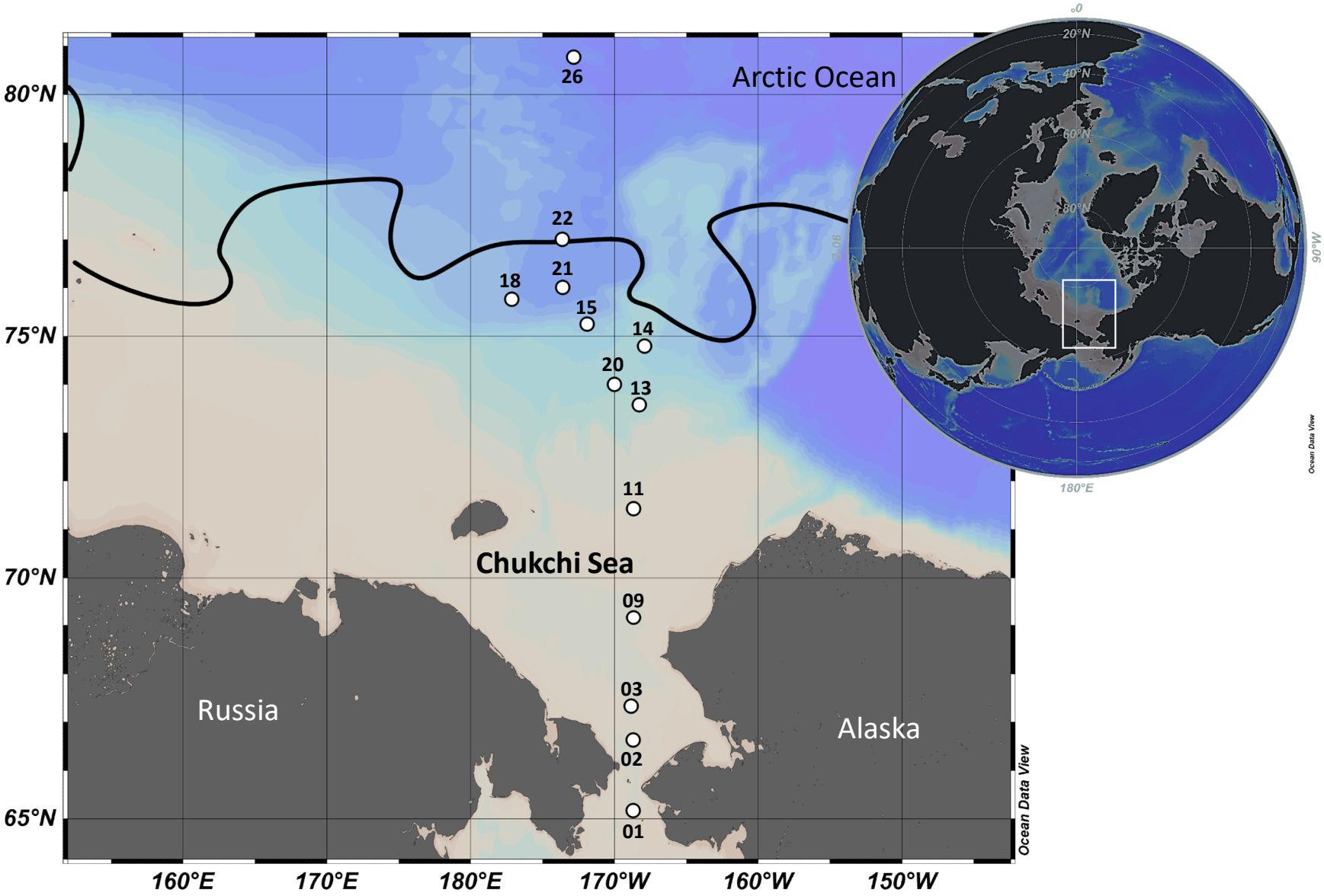

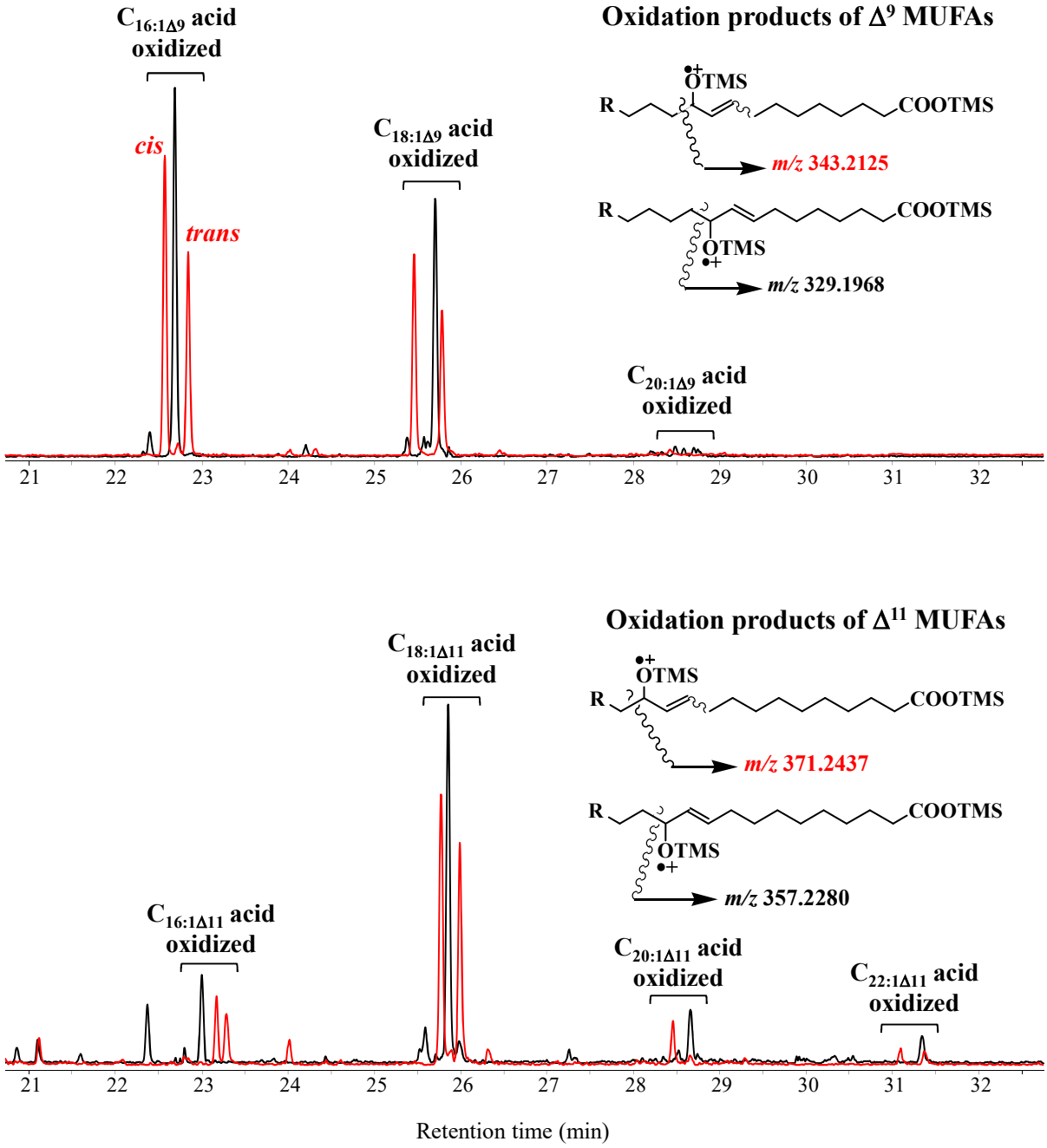

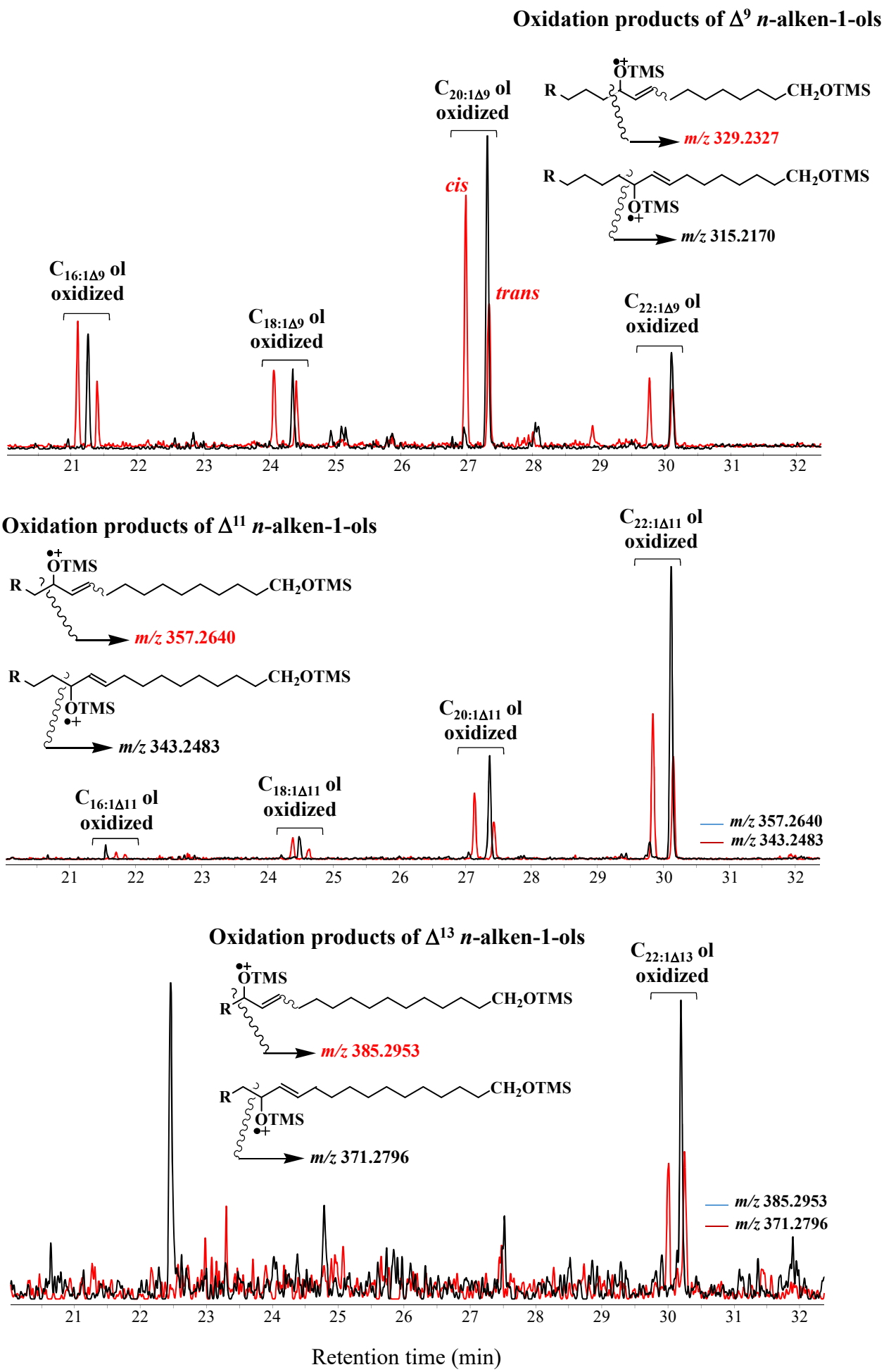

Figure

Click here to access/download;Figure;Figure 4.pdf

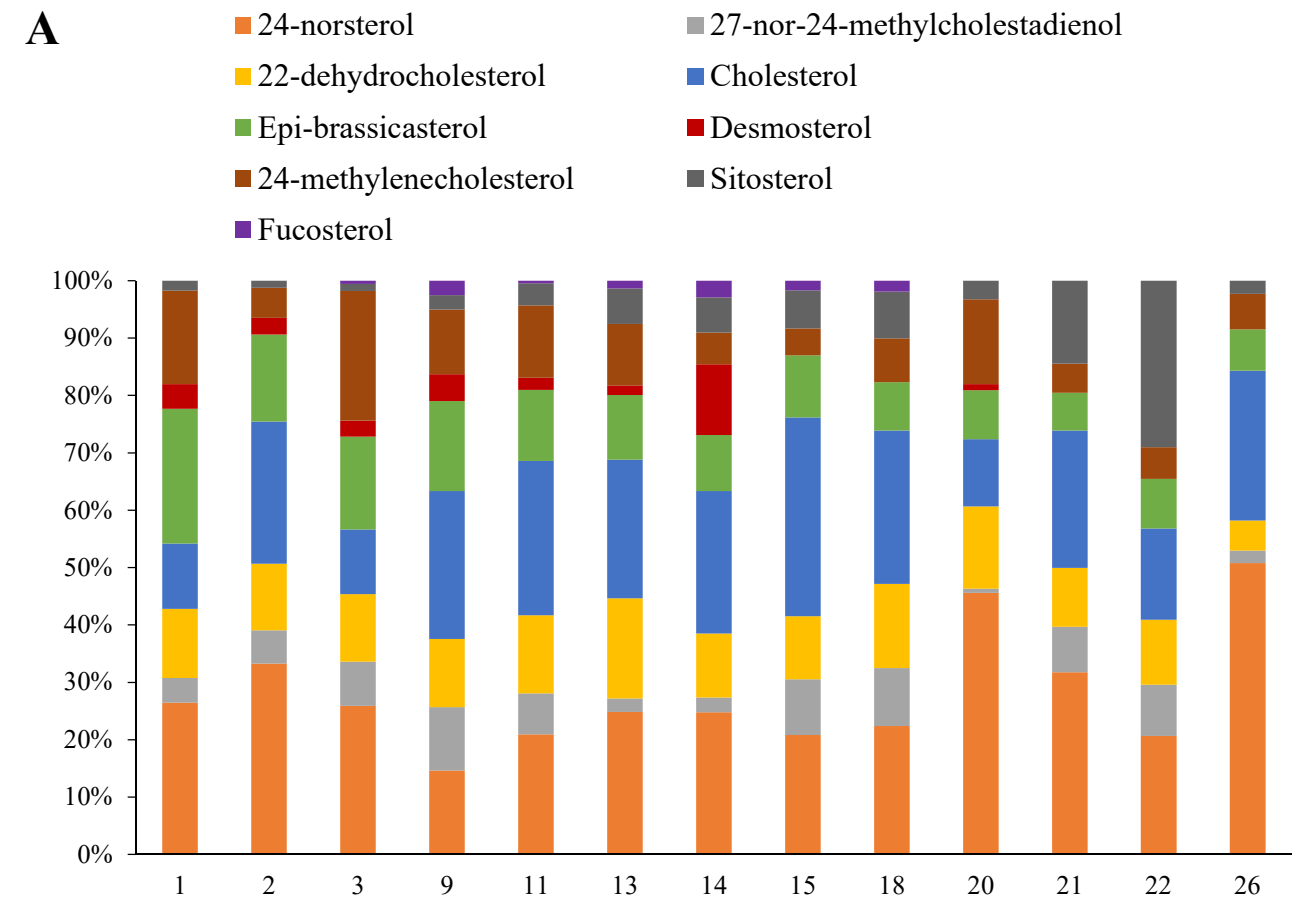

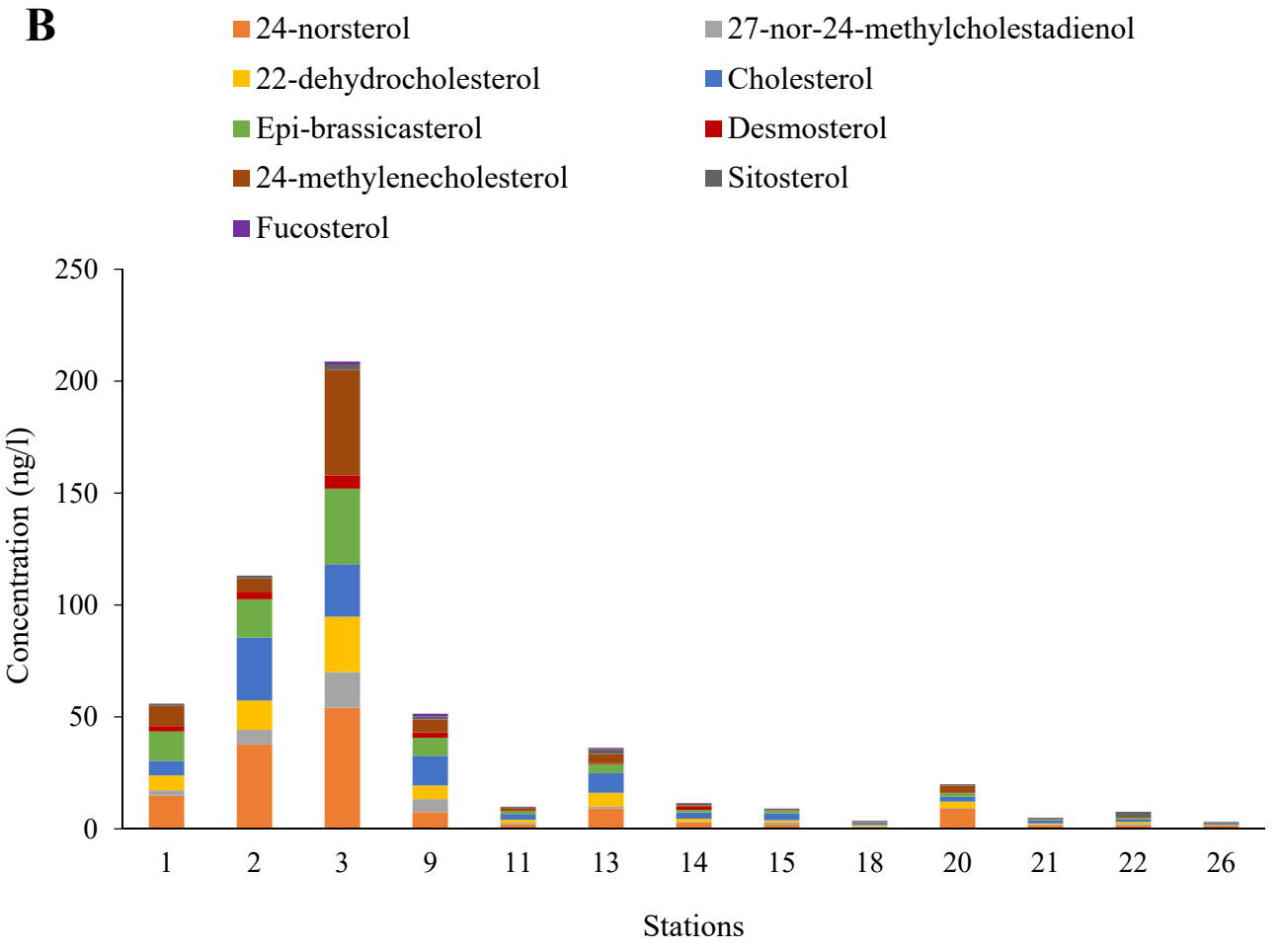

Figure

Click here to access/download;Figure;Figure 5.pdf

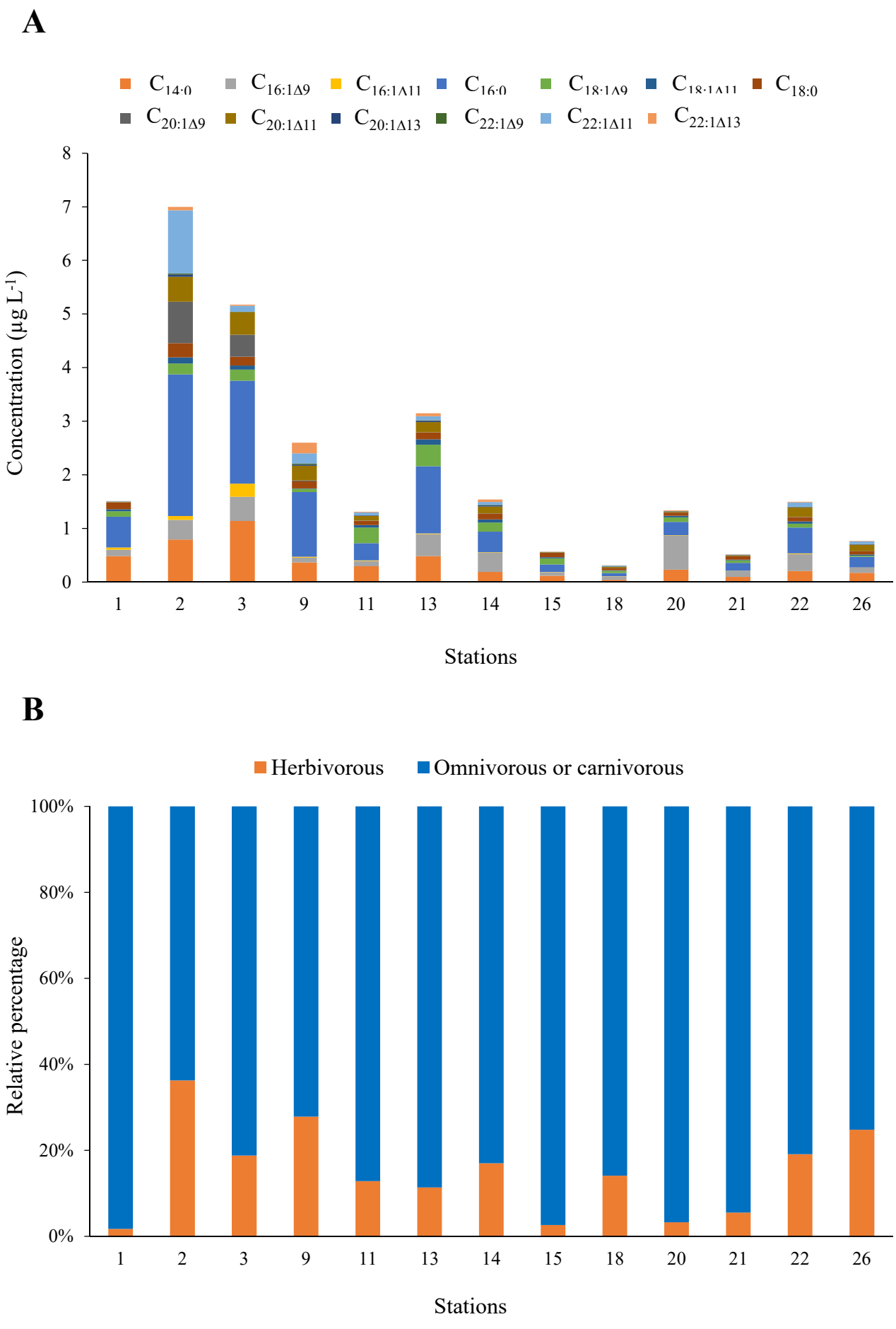

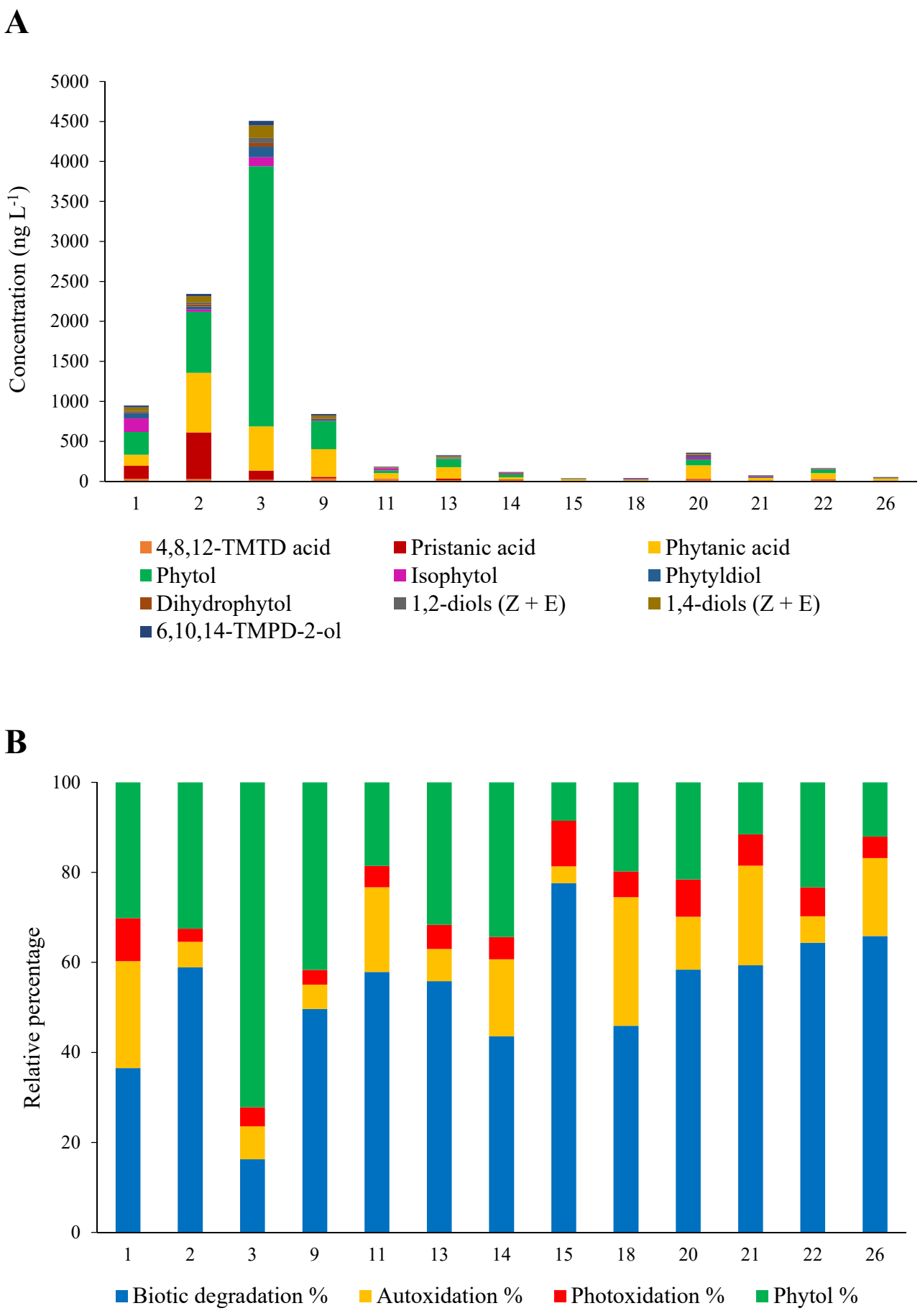

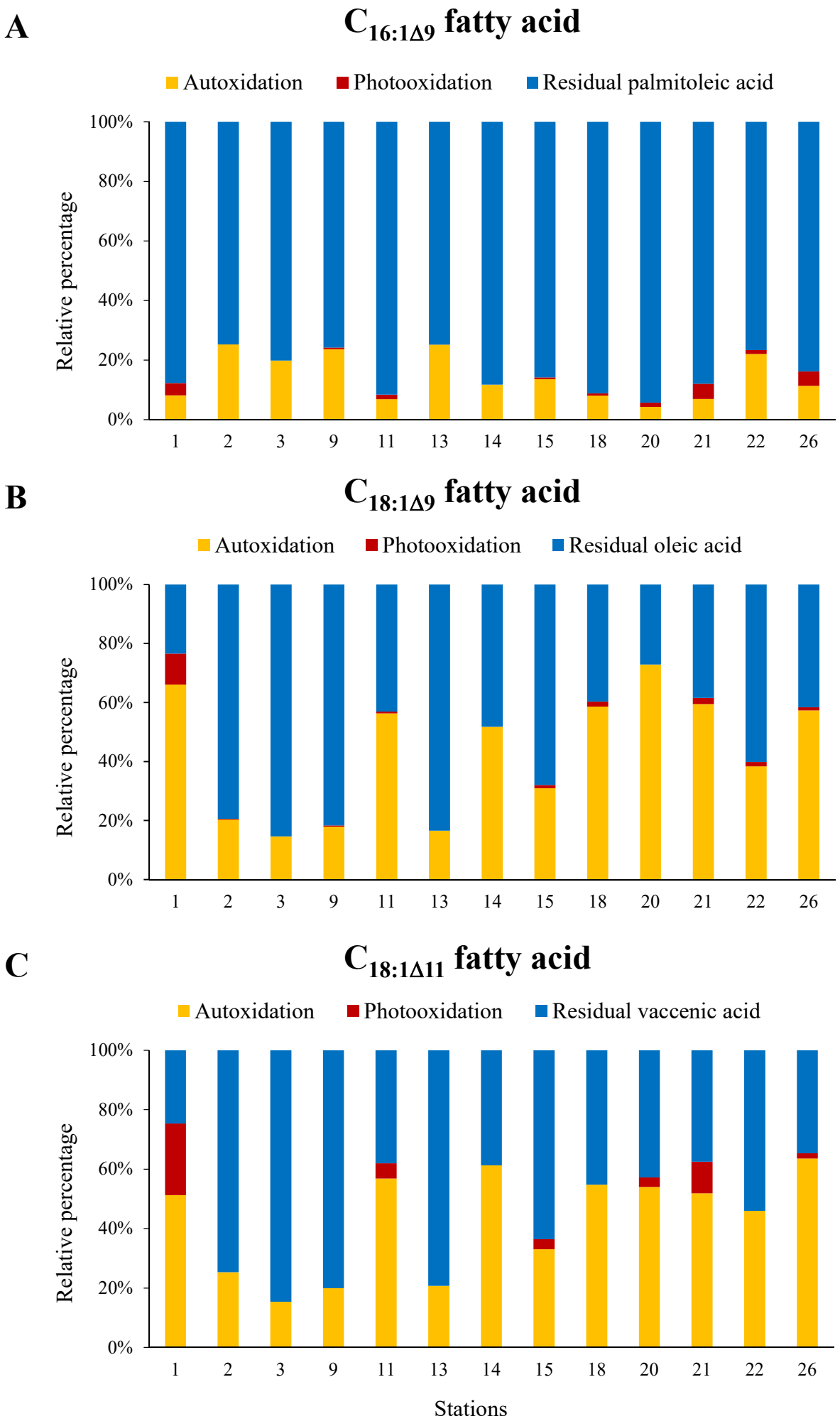

Figure

Click here to access/download;Figure;Figure 8.pdf

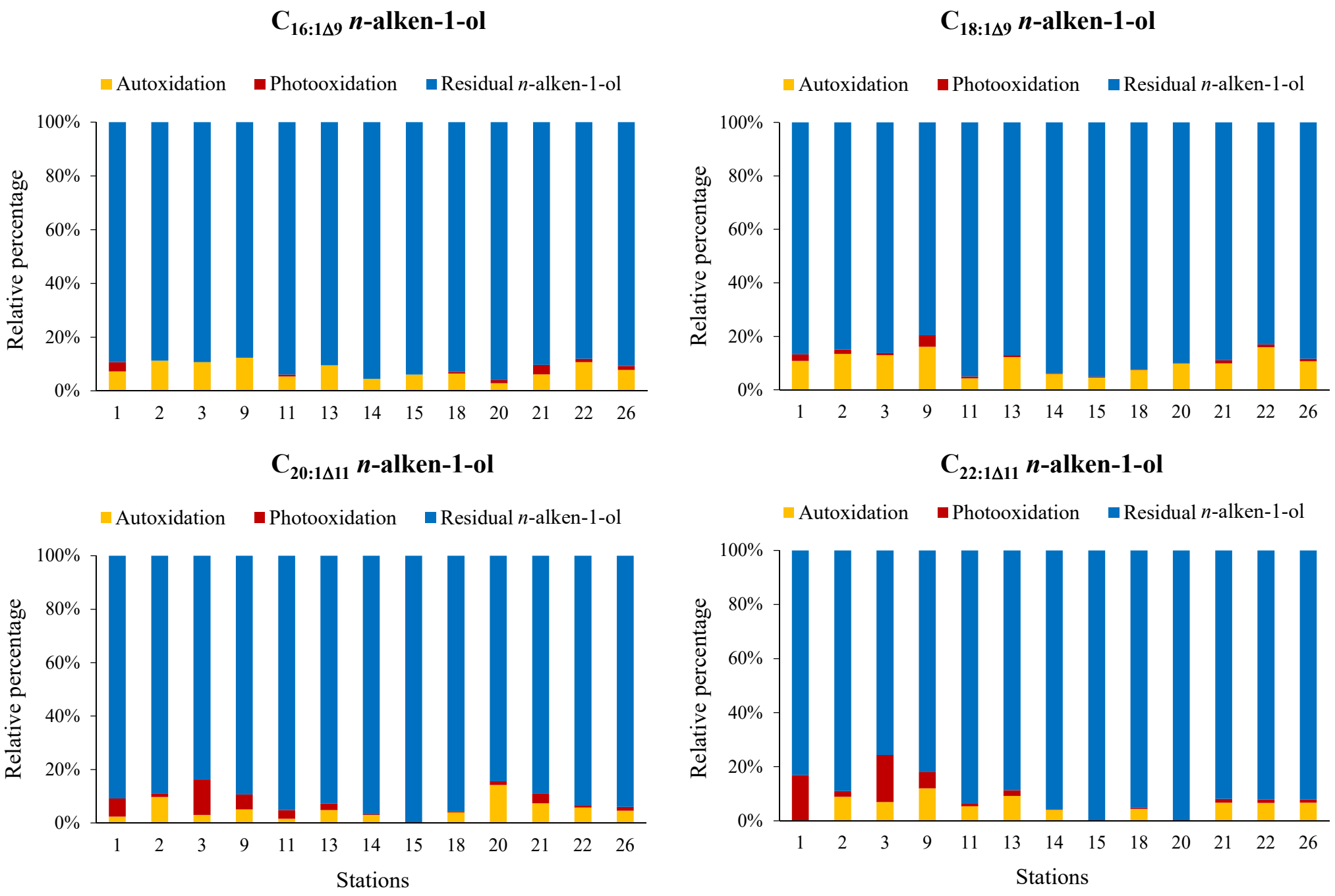

Figure

Click here to access/download;Figure;Figure 9.doc

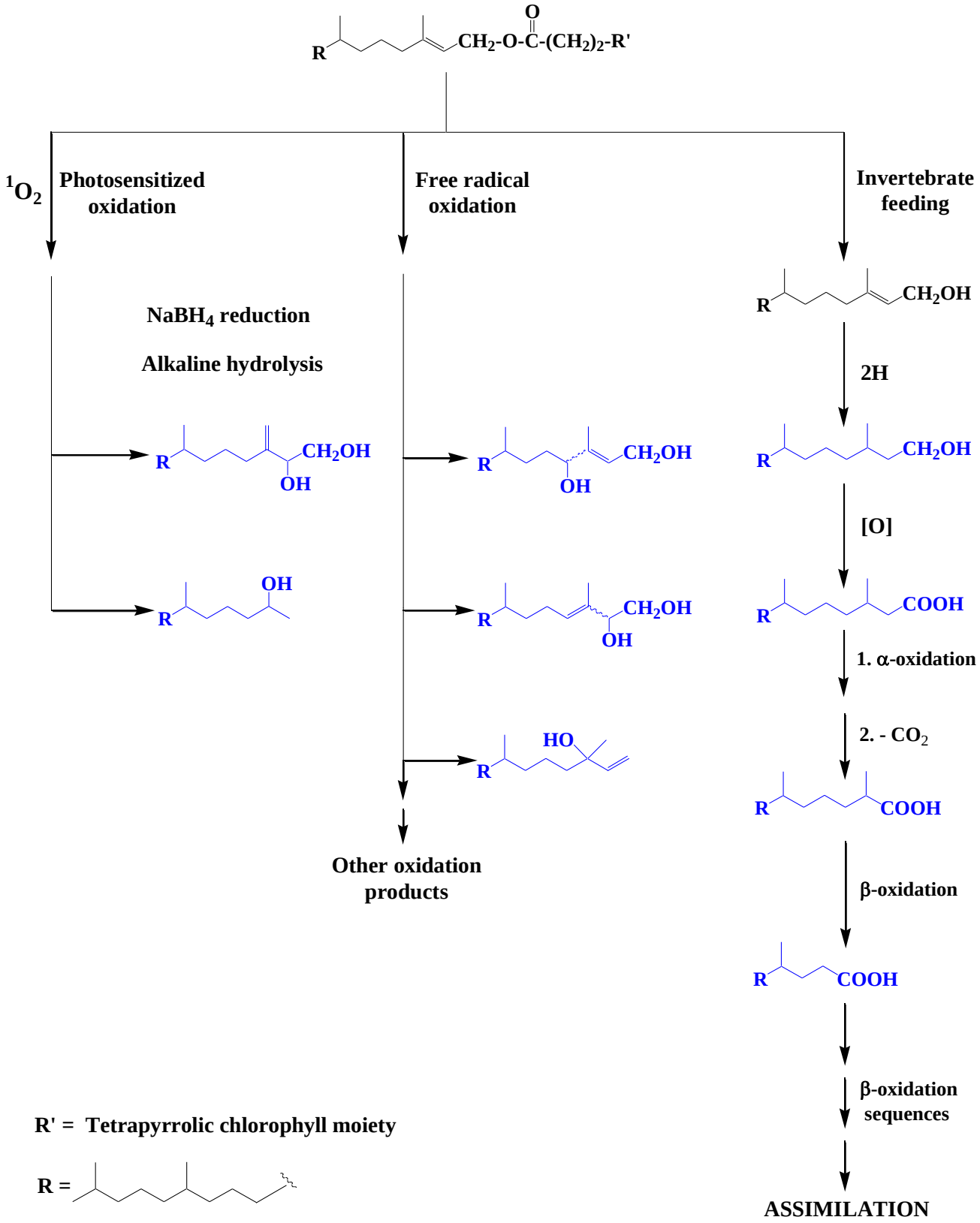

Table 1

Concentrations (ng L^{-1}) of the main sterols in the samples investigated.

Sterol	St 01	St 02	St 03	St 09	St 11	St 13	St 14	St 15	St 18	St 20	St 21	St 22	St 26
24-norcholesta-5,22*E*-dien-3β-ol	14.8	37.7	54.1	7.5	2.0	9.0	2.9	1.9	0.8	9.1	1.6	1.6	1.6
27-nor-24-methylcholesta-5,22-dien-3β-ol	2.4	6.5	16.0	5.7	0.7	0.9	0.3	0.9	0.4	0.1	0.4	0.7	0.1
Cholesta-5,22*E*-dien-3β-ol	6.7	13.1	24.6	6.1	1.3	6.3	1.3	1.0	0.5	2.9	0.5	0.9	0.2
Cholest-5-en-3β-ol	6.4	28.1	23.5	13.2	2.6	8.7	2.9	3.1	1.0	2.3	1.2	1.2	0.8
24-methylcholesta-5,22*E*-dien-3β-ol	13.1	17.1	33.8	8.1	1.2	4.1	1.1	1.0	0.3	1.7	0.3	0.7	0.2
Cholesta-5,24-dien-3β-ol	2.4	3.3	5.9	2.4	0.2	0.6	1.4	nd[a]	nd	0.2	nd	nd	nd
24-methylcholesta-5,24(28)-dien-3β-ol	9.1	6.0	47.1	5.8	1.2	3.9	0.6	0.4	0.3	3.0	0.2	0.4	0.2
24-ethylcholest-5-en-3β-ol	1.0	1.4	2.5	1.3	0.4	2.2	0.7	0.6	0.3	0.6	0.7	2.2	0.1
24(*E*)-ethylcholesta-5,24(28)-dien-3β-ol	nd	nd	1.2	1.3	0.1	0.5	0.3	0.2	0.1	nd	nd	nd	nd
Total	55.9	113.2	208.8	51.4	9.8	36.1	11.6	9.0	3.6	20.0	4.9	7.6	2.2

[a] nd = not detected (< 0.1 ng L^{-1})

Table 2

Concentrations (µg L^{-1}) of saturated and monounsaturated fatty acids in the samples investigated. PUFAs present in very weak proportion (reaching less than 4% at station 03) were not included in this table.

Station	$C_{14:0}$	$C_{16:1\Delta9}$	$C_{16:1\Delta11}$	$C_{16:0}$	$C_{18:1\Delta9}$	$C_{18:1\Delta11}$	$C_{18:0}$	$C_{20:1\Delta9}$	$C_{20:1\Delta11}$	$C_{20:1\Delta13}$	$C_{22:1\Delta9}$	$C_{22:1\Delta11}$	$C_{22:1\Delta13}$	Total
01	2.67	1.09	0.08	8.58	0.33	0.15	0.30	0.02	0.06	0.04	0.01	0.13	0.01	13.5
02	6.36	9.20	0.86	14.41	3.75	1.81	1.88	0.26	0.35	0.07	0.23	0.24	0.06	39.5
03	12.61	17.95	2.93	18.52	3.78	2.19	1.21	0.05	0.12	0.03	0.03	0.23	0.06	59.7
09	2.90	3.28	0.55	8.18	1.63	0.95	1.33	0.02	0.23	0.05	0.08	0.57	0.03	19.8
11	0.55	0.58	0.03	2.47	0.32	0.10	0.21	0.01	0.11	0.03	0.03	0.29	0.02	4.7
13	2.51	6.53	0.18	6.31	3.43	0.71	0.62	0.02	0.14	0.06	0.03	0.25	0.03	20.8
14	0.46	1.60	0.02	3.08	0.80	0.11	0.42	0.01	0.08	0.02	0.01	0.17	0.01	6.8
15	0.75	0.88	0.03	3.35	1.12	0.19	1.79	nd	0.02	0.01	nd	0.12	0.02	8.3
18	0.17	0.57	nd[a]	1.56	0.17	0.04	0.30	nd	0.03	0.01	0.01	0.30	0.01	3.3
20	1.47	8.97	nd	7.08	0.53	0.25	0.38	0.02	0.06	0.04	nd	0.12	0.02	18.9
21	0.52	1.10	0.02	2.58	0.25	0.05	0.27	nd	0.03	0.01	nd	0.18	0.01	5.0
22	1.57	5.64	0.10	4.69	2.14	0.27	0.89	nd	0.08	0.02	0.02	0.03	0.01	15.5
26	0.27	0.52	0.02	2.06	0.17	0.04	0.33	nd	0.05	0.01	0.02	0.04	0.01	3.5

[a] nd = not detected (< 0.01 µg L^{-1})

Table 4

Concentrations (µg L^{-1}) of *n*-alkan-1-ols in the samples investigated.

Compounds	St 01	St 02	St 03	St 09	St 11	St 13	St 14	St 15	St 18	St 20	St 21	St 22	St 26
$C_{14:0}$	0.24	0.40	0.57	0.18	0.15	0.24	0.10	0.06	0.02	0.12	0.05	0.10	0.09
$C_{16:1\Delta9}$	0.12	0.36	0.45	0.09	0.10	0.41	0.36	0.07	0.07	0.63	0.11	0.32	0.10
$C_{16:1\Delta11}$	0.04	0.07	0.24	0.02	0.01	0.01	0.01	0.01	nd[a]	0.01	0.01	0.01	nd
$C_{16:0}$	0.26	1.20	0.87	0.55	0.15	0.57	0.18	0.06	0.03	0.11	0.07	0.22	0.09
$C_{18:1\Delta9}$	0.10	0.20	0.21	0.06	0.29	0.40	0.17	0.11	0.04	0.08	0.05	0.07	0.02
$C_{18:1\Delta11}$	0.04	0.11	0.07	0.01	0.05	0.10	0.06	0.02	0.01	0.03	0.01	0.04	0.02
$C_{18:0}$	0.13	0.27	0.16	0.13	0.08	0.13	0.11	0.09	0.05	0.06	0.07	0.08	0.06
$C_{20:1\Delta9}$	0.01	0.77	0.41	0.02	nd	nd	nd	nd	nd	nd	nd	nd	nd
$C_{20:1\Delta11}$	0.02	0.46	0.42	0.28	0.09	0.19	0.13	0.01	0.02	0.01	0.01	0.17	0.11
$C_{20:1\Delta13}$	nd	0.04	nd	0.02	0.01	0.02	0.02	nd	nd	nd	nd	0.01	0.01
$C_{22:1\Delta9}$	nd	0.02	0.01	0.02	nd	0.01	0.01	nd	nd	0.01	nd	0.01	0.01
$C_{22:1\Delta11}$	0.01	1.18	0.11	0.19	0.05	0.07	0.06	nd	0.02	nd	0.01	0.08	0.05
$C_{22:1\Delta13}$	nd	0.06	0.02	0.20	0.01	0.05	0.05	nd	nd	0.01	nd	0.01	0.01
Total	0.96	5.16	3.56	1.76	0.99	2.22	1.24	0.43	0.26	1.09	0.38	1.13	0.58

[a] nd = not detected (< 0.01 µg L^{-1})

Table S1

Coordinates and sampling dates of the different stations sampled.

Station	Sampling date	Latitude (°N)	Longitude (°W)
01	02/08/2015	65.173	168.690
02	02/08/2015	66.630	168.688
03	02/08/2015	67.333	168.834
09	03/08/2015	69.167	168.668
11	04/08/2015	71.430	168.670
13	04/08/2015	73.581	168.283
14	05/08/2015	74.798	167.899
15	05/08/2015	75.250	171.901
18	07/08/2015	75.761	177.152
20	08/08/2015	76.007	173.608
21	08/08/2015	73.999	169.997
22	09/08/2015	77.006	173.617
26	13/08/2015	80.774	172.849

Table 3

Concentrations of isoprenoid compounds, chlorophyll and chlorophyll photooxidation estimates in the samples investigated.

	St 01	St 02	St 03	St 09	St 11	St 13	St 14	St 15	St 18	St 20	St 21	St 22	St 26
3,7,11,15-tetramethylhexadec-2-en-1-ol (Phytol)[a]	286	762	3253	351	34	104	40	3	8	77	9	39	6
4,8,12-trimethytridecanoic acid (4,8,12-TMTD acid)[a]	29	28	20	35	33	17	19	4	6	18	10	20	8
2,6,10,14-tetramethylpentadecanoic acid (Pristanic acid)[a]	167	585	113	20	4	17	4	3	1	11	3	7	2
2,6,10,14-tetramethylhexadecanoic acid (Phytanic acid)[a]	139	745	553	346	64	143	26	20	10	169	30	77	23
3,7,11,15-tetramethylhexadec-1-en-3-ol (Isophytol)[a]	169	27	113	7	28	3	12	nd[e]	9	27	15	1	7
3-methylidene-7,11,15-trimethylhexadecan-1, 2-diol[a]	68	39	134	10	3	5	1	1	1	18	2	5	1
3,7,11,15-tetramethylhexadecan-1-ol (Dihydrophytol)[a]	14	24	46	17	4	7	1	2	1	10	2	4	1
3,7,11,15-tetramethylhexadec-3-en-1,2-diols (*Z* and *E*)[a]	10	29	61	10	2	5	2	1	1	5	1	2	1
3,7,11,15-tetramethylhexadec-2-en-1,4-diols (*Z* and *E*)[a]	46	77	156	28	5	15	5	1	2	10	1	6	1
6,10,14-trimethylpentadecan-2-ol[a]	23	30	59	18	6	12	4	3	2	12	3	6	2
Total	951	2346	4508	842	183	328	114	38	41	357	76	167	52
CPPI[b]	0.191	0.041	0.033	0.022	0.072	0.041	0.028	0.173	0.071	0.187	0.180	0.096	0.104
Chlorophyll[c]	2.50	2.01	7.17	0.68	0.27	0.29	0.16	0.04	0.06	1.01	0.09	0.13	0.11
Chlorophyll photooxidation estimate (%)[d]	96.1	52.7	45.3	33.0	72.2	52.8	40.5	94.8	71.8	95.8	95.4	81.5	84.0

[a] (ng L^{-1})

[b] Chlorophyll Phytyl side-chain Photooxidation Index (molar ratio 3-methylidene-7,11,15-trimethylhexadecan-1,2-diol /phytol)

[c] (µg L^{-1})

[d] Estimated with the empirical equation: chlorophyll photodegradation % = $(1 - [CPPI + 1]^{-18.5}) \times 100$ (Cuny et al. 2002).

[e] nd = not detected (< 1 ng L^{-1})

Table S2

Accurate masses of the main fragment ions produced during EI fragmentation of silylated monounsaturated fatty acid autoxidation products.

Parent fatty acid	*m/z*	*m/z*	*m/z*	*m/z*
$C_{16:1\Delta9}$	199.1518[a]	213.1675[a]	329.1968[b]	343.2125[b]
$C_{16:1\Delta11}$	171.1206	185.1363	357.2280	371.2437
$C_{16:1\Delta13}$	143.0748	157.1051	385.2592	399.2749
$C_{18:1\Delta9}$	227.1830	241.1987	329.1968	343.2125
$C_{18:1\Delta11}$	199.1518	213.1675	357.2280	371.2437
$C_{18:1\Delta13}$	171.1206	185.1363	385.2592	399.2749
$C_{20:1\Delta9}$	255.2139	269.2295	329.1968	343.2125
$C_{20:1\Delta11}$	227.1830	241.1987	357.2280	371.2437
$C_{20:1\Delta13}$	199.1518	213.1675	385.2592	399.2749
$C_{22:1\Delta9}$	283.2451	297.2607	329.1968	343.2125
$C_{22:1\Delta11}$	255.2139	269.2295	357.2280	371.2437
$C_{22:1\Delta13}$	227.1830	241.1987	385.2592	399.2749

[a] Fragments containing the terminal methyl group.

[b] Fragments containing the trimethylsilyl ester group.

Table S3

Accurate masses of the main fragment ions produced during EI fragmentation of silylated monounsaturated *n*-alken-1-ol autoxidation products.

Parent *n*-alkenol	*m/z*	*m/z*	*m/z*	*m/z*
$C_{16:1\Delta9}$	199.1518[a]	213.1675[a]	315.2170[b]	329.2327[b]
$C_{16:1\Delta11}$	171.1206	185.1363	343.2483	357.2640
$C_{16:1\Delta13}$	143.0748	157.1051	371.2796	385.2953
$C_{18:1\Delta9}$	227.1830	241.1987	315.2170	329.2327
$C_{18:1\Delta11}$	199.1518	213.1675	343.2483	357.2640
$C_{18:1\Delta13}$	171.1206	185.1363	371.2796	385.2953
$C_{20:1\Delta9}$	255.2139	269.2295	315.2170	329.2327
$C_{20:1\Delta11}$	227.1830	241.1987	343.2483	357.2640
$C_{20:1\Delta13}$	199.1518	213.1675	371.2796	385.2953
$C_{22:1\Delta9}$	283.2451	297.2607	315.2170	329.2327
$C_{22:1\Delta11}$	255.2139	269.2295	343.2483	357.2640
$C_{22:1\Delta13}$	227.1830	241.1987	371.2796	385.2953

[a] Fragments containing the terminal methyl group.

[b] Fragments containing the terminal trimethylsilyl ether group.